Adv Polym Sci (2005) 186: 211–254
DOI 10.1007/b136821

Published online: 1 September 2005

# Analysis of Polysaccharides by Ultracentrifugation. Size, Conformation and Interactions in Solution

Stephen E. Harding

NCMH Physical Biochemistry Laboratory, University of Nottingham, School of Biosciences, Sutton Bonington LE12 5RD, UK
*Steve.Harding@nottingham.ac.uk*

**1 Introduction** . . . 212

**2 Types of Sedimentation Analysis** . . . 214

**3 Instrumentation** . . . 215

**4 Polysaccharide Polydispersity and Simple Shape Analysis by Sedimentation Velocity** . . . 219
4.1 Sedimentation Coefficient Distributions: DCDT and SEDFIT . . . 221
4.2 Time Derivative Analysis: DCDT . . . 221
4.3 Lamm Equation Approach: SEDFIT . . . 223
4.4 Molecular Weight and Conformation . . . 225

**5 Polysaccharide Molecular Weight Analysis by Sedimentation Equilibrium** . . . 227
5.1 Molecular Weight Information Obtained . . . 228
5.2 Obtaining the Weight Average Molecular Weight: MSTAR . . . 228
5.3 Correcting for Thermodynamic Non-Ideality: Obtaining $M_w$ from $M_{w,app}$ . . . 232
5.4 Distributions of Molecular Weight . . . 234
5.5 Number and *z*-Averages: Polydispersity Index . . . 234
5.6 SEC/MALLs and the New Role of Sedimentation Equilibrium . . . 235

**6 Polysaccharide Conformation Analysis** . . . 236
6.1 The Wales–van Holde Ratio . . . 236
6.2 Power Law or Scaling Relations . . . 237
6.2.1 General Conformation: Haug Triangle and Conformation Zoning . . . 238
6.3 Rigid Cylindrical Structures . . . 239
6.4 Semi-Flexible Chains: Worm-Like Coils . . . 241

**7 Associative Interactions** . . . 242
7.1 Polysaccharide Mucoadhesive Interactions . . . 243
7.2 Mucoadhesion Involving Guar, Alginate, Carboxymethyl Cellulose, Xanthan and DEAE-Dextran . . . 244
7.3 Mucoadhesion Experiments Involving Chitosans . . . 244
7.4 Effect of the Environment on the Extent of Interaction . . . 246
7.5 Sedimentation Fingerprinting . . . 246
7.6 Measurement of Charge and Charge Screening . . . 247

**8 Comment** . . . 249

**References** . . . 249

**Abstract** The launch of the XL-I analytical ultracentrifuge by Beckman Instruments (Palo Alto, USA) in 1996 and subsequent development of penetrating software for the analysis of the optical records digitally recorded in this new generation instrument has made some exciting possibilities for the analysis of polysaccharides in a solution environment. We review these developments and investigate the application of the technique to the study of polysaccharide polydispersity, molecular weight analysis, conformation and flexibility analysis, the study of associative interactions, including large complex formation phenomena, and to the measurement of charge and charge-shielding phenomena.

**Keywords** Complex · Flexibility · Molecular weight distribution · Mucoadhesion · Sedimentation coefficient distribution

## 1 Introduction

The enhancement of our knowledge of the biophysical properties of polysaccharides in dilute and concentrated solution form is important for both our understanding of their function on a "macroscopic" scale in nature, and how they can be used and manipulated by Industry and Medicine [1]. In the *Food Industry* for example such biophysical information—namely molecular size, shape, polydispersity and interaction properties—alongside chemical composition data, is important for the proper understanding of polysaccharide behaviour as gelling agents, thickeners and as phase separation media. This information used alongside economic considerations can help us choose the right polysaccharide with the right properties for a particular product. The same is true for the *Pharmaceutical and Healthcare Industries*: this may be for example in the choice of the right polysaccharide as an encapsulation agent, as a mucoadhesive or slow release formulation in drug delivery, as a viscosity enhancer in toothpaste, eye and nose drops or as a film former in hair products. In the *Printing Industry*, knowledge of biophysical properties can help us choose the right polysaccharide for producing good clear print quality, and in the *Oil Industry* it facilitates the choice of the most suitable polysaccharide as a lubricant and water immobilisation agent. In *Medicine* the choice of the right dextran as a blood plasma substitute is strongly dictated by molecular weight considerations.

There are several techniques now at our disposal for obtaining this fundamental biophysical information about solutions of polysaccharides (Table 1 [2–7]), but as is well known these substances are by no means easy to characterise. These difficulties arise from their highly expanded nature in solution, their polydispersity, (not only with respect to their molecular weight but also for many with respect to composition), the large variety of conformation and in many cases their high charge and in some their ability to stick together [1, 8]. All of these features can complicate considerably the interpretation of solution data.

**Table 1** Hydrodynamic techniques for characterising the biophysical properties of polysaccharides in solution

| Technique | Biophysical information | Comment | Ref. |
|---|---|---|---|
| Analytical ultracentrifugation (AUC) | Molecular weight $M$, molecular weight distribution, $g(M)$ vs. $M$, polydispersity, sedimentation coefficient, $s$, and distribution, $g(s)$ vs. $s$: solution conformation and flexibility. Interaction & complex formation phenomena. Molecular charge | No columns or membranes required | [2] |
| Static (multi-angle laser) light scattering (SLS or MALLs) | Molecular weight, radius of gyration, $R_g$: solution conformation and flexibility. | Solutions need to be clear of supramolecular aggregates. $R_g$ more sensitive to conformation than $s$. | [3] |
| Size exclusion chromatography coupled to static light scattering (SEC-MALLs) | Molecular weight, molecular weight distribution. Polydispersity. Radius of gyration and distribution: solution conformation and flexibility. | Method of choice for molecular weight work. | [4] |
| Dynamic light scattering (DLS) | Translational diffusion coefficient, hydrodynamic or Stokes radius $R_h$: branching information (when $R_h$ used with $R_g$) | Fixed 90° angle instruments not suitable for polysaccharides, Multi-angle instrument necessary. | [3] |
| Small angle X-ray scattering | $R_g$, chain contour length, $L$: solution conformation and flexibility | If $M$ is also known, can provide mass per unit length $M_L$ | [5] |
| Viscometry | Intrinsic viscosity $[\eta]$: conformation and flexibility. | $[\eta]$, like $R_g$, much more sensitive than $s$. Accurate concentration estimates required. | [6] |
| Surface plasmon resonance (SPR) | Interaction strength (molar dissociation constant, $K_d$). | One member of the reacting pair needs to be immobilised onto an "inert" surface. Not suitable for self-association analysis. | [7] |

In this article we choose to focus on analytical ultracentrifugation as a primary method for obtaining fundamental physical information about polysaccharides in solution mainly because of its diversity, its absolute nature and inherent fractionation ability without the need for separation columns or membranes [2]. We will consider the salient features behind the modern delivery of the various types of sedimentation analysis, the instrumentation involved and analysis software, and we will indicate where combination with the other solution techniques listed in Table 1 is appropriate, as well as with imaging techniques like electron microscopy and atomic force microscopy. We refrain from unnecessary mathematical detail which would otherwise render the description opaque to the non-specialist reader but instead provide the source references where such detail can be found. The main polysaccharides we will use as examples are two neutral groups of polysaccharide, namely starch (amylose and amylopectin), galactomannans (guar gum, tara gum and locust bean gum) and some polyelectrolytes, namely the polyanionic heparin and the polycationic chitosan group (of various degrees of acetylation).

## 2 Types of Sedimentation Analysis

What sort of information can we obtain about polysaccharides in solution from sedimentation analysis in analytical ultracentrifuge? The information obtained depends on the type of sedimentation technique we apply—all possible with the same instrumentation [9–12]. *Sedimentation velocity* can provide us with information on the physical homogeneity of a sample, conformation and flexibility information—in some cases to surprising detail. It can also provide us with interaction information if, for example we assay for what is called "co-sedimentation" phenomena (i.e. species sedimenting at the same rate as another). At lower rotor speeds, *sedimentation equilibrium* can provide absolute molecular weight and molecular weight distribution information, supplementing the more popular technique (for polysaccharides) of size exclusion chromatography coupled to multi-angle laser light scattering: SEC/MALLs [13]. Another recent postulated use for the analytical ultracentrifuge is the *measurement of the molecular charge* on polysaccharides in solution, and this will also be considered [14].

There are two other adaptations of the analytical ultracentrifuge of relevance to polysaccharides: one is *gel sedimentation analysis* for the measurement of swelling pressures and related rheological parameters. Another is *diffusion analysis through matrices and interfaces*: although dynamic light scattering is now popularly used for the measurement of translational diffusion coefficients, the optical system on the analytical ultracentrifuge is

proving very useful for the investigation of the diffusion of molecules through matrices, and towards and through interfaces between incompatible two phase systems (including aqueous two-phase polysaccharide systems). In this article—which focuses on the biophysical properties of polysaccharides in solution—we will not consider gel sedimentation or matrix/interface diffusion: both have been covered by two other recent and extensive reviews, both appearing in *Biotechnology and Genetic Engineering Reviews* [15, 16]. The actual formation of membranes at interfaces can also be followed by synthetic boundary methods in the ultracentrifuge, and this has been dealt with in a recent article by C. Wandrey and colleagues [17].

## 3 Instrumentation

An analytical ultracentrifuge (Fig. 1) is simply an ultracentrifuge with an appropriate optical system and data-capture facility for observing and recording solute distributions both during and at the end of the sedimentation process. The analytical ultracentrifuge is by no means a new concept—Svedberg's first oil-turbine driven instrument dates from the early 1920s. It is worth noting that Svedberg and his students subsequently published several papers on polysaccharides: these were mainly in the 1940s and were mostly on cellulose and cellulose derivatives (see [18] and references sited therein). The boom period of the technique was 1940–1970 with several commercially available analytical ultracentrifuges available, most notably the Beckman (Palo Alto, USA) Model E (see [19] and references therein). From the late 1970s analytical ultracentrifuges no longer became commercially available on the western side of the Iron Curtain (apart from a crude Schlieren adaptor for a Beckman L8

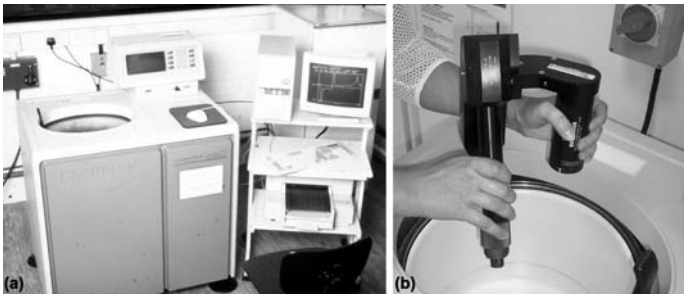


**Fig. 1** A modern analytical ultracentrifuge. **a** Beckman Optima XLA/I, with full on-line data capture and analysis facility. **b** Its UV/visible monochromator and, for interference optics, the laser light source are contained in the rotor chamber and have to be installed and removed at the start/end of each run

preparative ultracentrifuge). In Eastern Europe the Hungarian Optical Works in Budapest continued to manufacture their high quality MOM analytical ultracentrifuge [20]. Following the collapse of the Berlin Wall in 1990 a new generation instrument appeared in the form of the Beckman Optima XLA ultracentrifuge, with on-line ultra-violet(UV)/visible absorption optics, giving a direct record of solute concentration (in absorption units), $c(r)$ versus radial displacement $r$ [21]. This, however, had limited relevance for polysaccharides because of the lack of chromophore these substances possess in the near-UV (250–300 nm) and visible region. Chemical addition of a chromophore label permitted its use. Studies on two labelled dextrans: "blue" dextran (Cibacron Blue F3GA-dextran) [22] and di-iodotyrosine dextran [23] demonstrated that under these circumstances the UV absorption optical system on an analytical ultracentrifuge could successfully be used for measurements of sedimentation coefficient and molecular weight: with the latter substance some alteration in dextran conformation induced by the chromophore was evident. Those studies, however, were performed on the older MSE Centrican analytical ultracentrifuge. The first use of an XLA ultracentrifuge for the characterisation of a polysaccharide was by H. Cölfen and colleagues in 1996 who used an XLA to characterise the sedimentation coefficient and molecular weight of two chitosans labelled with the fluorophore 9-anthraldehyde [24]. This was subsequently followed by the launch by Beckman of the XLI ultracentrifuge with integrated refractive index (Rayleigh Interference) and UV/visible optics [25]: application to polysaccharides became possible on a routine basis.

The laser (wavelength 670 nm) on the XL-I instrument provides high-intensity, highly collimated light and the resulting interference patterns (between light passing through the solution sector and reference solvent sector of an ultracentrifuge cell) are captured by a CCD camera. A Fourier transformation converts the interference fringes into a record of concentration $c(r) - c(a)$ relative to the meniscus ($r = a$) as a function of radial displacement $r$ from the axis of rotation. The measurement is in terms of Rayleigh fringe units relative to the meniscus, $j(r)$, with $J(r) = j(r) + J(a)$, $J(r)$ being the absolute fringe displacement and $J(a)$ the absolute fringe displacement at the meniscus. For a standard optical path length cell ($l = 1.2$ cm) with laser wavelength $\lambda = 6.70 \times 10^{-5}$ cm, a simple conversion exists from $J(r)$ in "fringe shift" units to $c(r)$ in g/ml:

$$\begin{aligned} c(r) &= J(r)\lambda/\{(\mathrm{d}n/\mathrm{d}c)l\} \\ &= \{5.58 \times 10^{-5}/(\mathrm{d}n/\mathrm{d}c)\}J(r) \end{aligned} \tag{1}$$

with similar conversions for $j(r)$ and $J(a)$. $\mathrm{d}n/\mathrm{d}c$ is the (specific) refractive index increment, which depends on the polysaccharide, solvent and wavelength. A comprehensive list of values for a range of macromolecules has recently been published [26]. Some of the values taken from [26] for polysaccharides are listed in Table 2: it can be seen that in aqueous systems most

**Table 2** Refractive index increments of some polysaccharides (data taken from [26] and references cited therein). DS: degree of substitution. λ: wavelength

| Polysaccharide | Solvent | λ (nm) | Temp (°C) | d*n*/d*c* (ml/g) |
|---|---|---|---|---|
| Alginate (magnesium) | $MgCl_2$ (aq.) | 546 | 20–25 | 0.158 |
| Alginate (potassium) | Aq. solution | 546 | 20–25 | 0.165 |
| Alginate (sodium) | Aq. solution | 546 | 20–25 | 0.165 |
| Amylopectin | DMSO/ water (90/10 w/w) | 632.8 | 25 | 0.074 |
| Amylose | DMSO/water (50/50 vol) | 546 | 25 | 0.112 |
| Amylose | DMSO/water (90/10 vol) | 546 | 25 | 0.062 |
| Amylose | 4.2M GuHCl | 546 | 25 | 0.118 |
| Amylose acetate | Nitromethane | 436 | 20 | 0.0835 |
| Amylose tributyrate | Ethyl acetate | 546 | 25 | 0.098 |
| Amylose tricarbaanilate | Acetone | 546 | 27 | 0.228 |
| Amylose tripropionate | Ethyl acetate | 546 | 25 | 0.092 |
| Beta-glucan | Water | 488 | 25 | 0.151 |
| Carboxymethyl cellulose (several DS) | 0.1 M $NaNO_3$ | 632.8 | 25 | 0.163 |
| Cellulose | Acetone | 546 | 25 | 0.111 |
| Cellulose diacetate | Acetone | 546 | 25 | 0.112 |
| Cellulose nitrate (12.9% N) | Acetone | 546 | 25 | 0.115 |
| Cellulose nitrate (14.0% N) | Acetone | 436 | 25 | 0.09 |
| Cellulose propionate | Acetone | 632.8 | 25 | 0.111 |
| Cellulose propionate | MEK | 632.8 | 25 | 0.096 |
| Cellulose tributyrate | DMF | 546 | 41 | 0.0442 |
| Cellulose tricaproate | DMF | 546 | 41 | 0.0442 |
| Cellulose tricarbanilate | Acetone | 546 | 27 | 0.218 |
| Cellulose tricarbanilate | Dioxane | 546 | 25 | 0.165 |
| Cellulose trinitrate | Acetone | 546 | 25 | 0.112 |
| Cellulose trinitrate | Ethyl acetate | 546 | 30 | 0.102 |
| Chitosan | Acetate buffer | 633 | 25 | 0.181* |
| Dextran | Acetate buffer | 633 | 25 | 0.150 |
| Dextran | Water | 436 | 25 | 0.152 |
| Dextran | NaCl (aq.) | 436 | 25 | 0.136 |
| Dextran | 0.5 M NaCl | 546 | 25 | 0.147 |
| Dextran | 1.0 M NaCl | 546 | 25 | 0.144 |
| Ethyl cellulose | Methanol | 546 | 25 | 0.13 |
| Gum arabic | HCl (aq.) | 436 | 25 | 0.152 |
| Heparin (various commercial) | Acetate buffer | 690 | 25 | 0.129–0.134 |
| Hyaluronic acid | Water | 546 | 25 | 0.166–0.170 |
| Hydroxypropyl cellulose | Water | 546 | 25 | 0.146 |
| Hydroxypropyl cellulose | Water | 578 | 25 | 0.143 |
| Hydroxypropyl starch (DS 0.5) | Water | 546 | 20 | 0.152 |

**Table 2** (continued)

| Polysaccharide | Solvent | λ (nm) | Temp (°C) | d$n$/d$c$ (ml/g) |
|---|---|---|---|---|
| Hydrolysed waxy maize starch (amylopectin) | Water | 546 | 20 | 0.152 |
| Kappa-carrageenan | 0.1 M LiCl | 633 | 25 | 0.111 |
| Kappa-carrageenan | 0.1 M LiCl | 633 | 60 | 0.115 |
| Pectin (citrus) | Water | 633 | 25 | 0.146 |
| Pullulan | Phosphate buffer | 633 | 30 | 0.137 |
| Schizophyllan | Water | 546 | 25 | 0.145 |
| Sodium carboxymethyl amylose | 0.35 M NaCl | 546 | 35 | 0.133 |

* depends on the degree of acetylation

**Table 3** Refractive index increment and partial specific volume of hyaluronan ($M \sim 10^5$ g/mol) determined at different salt concentrations (from [28])

| Solvent NaCl (mol $l^{-1}$) | Refractive index increment (ml/g) | | | Partial specific volume (ml/g) |
|---|---|---|---|---|
| | 436 nm | 546 nm | 633 nm | |
| 0.25 | 0.167 | 0.165 | 0.164 | 0.57 |
| 0.20 | 0.167 | 0.165 | 0.164 | 0.57 |
| 0.05 | 0.168 | 0.166 | 0.165 | 0.56 |
| 0.01 | 0.171 | 0.168 | 0.166 | 0.53 |
| 0.005 | 0.172 | 0.169 | 0.167 | 0.51 |
| 0.001 | 0.178 | 0.175 | 0.173 | 0.47 |

values lie between 0.14–0.16 ml/g, although for non-aqueous systems the values can range enormously from 0.044–0.218 ml/g. The data for example for $\kappa$-carrageenan suggest little temperature dependence although that for dextrans suggests a significant dependence on wavelength. A study on the polycationic chitosan [27] suggested that the degree of substitution of some polysaccharides can strongly influence d$n$/d$c$, particularly if ionic groups are involved. Preston and Wik [28] have explored in detail the effect of ionic strength and wavelength on d$n$/d$c$ for the polyanion hyaluronate (Table 3). These results show that if a user needs, for whatever reason, an accurate value for d$n$/d$c$ for a polysaccharide he should measure it directly in the particular buffer used for the ultracentrifuge experiments. It is worth emphasising that converting fringe shift concentrations {$j(r)$ or $J(r)$} to weight concentrations is not normally necessary for most applications. In addition, for sedimentation velocity work it is possible to work with $j(r)$ or $c(r) - c(a)$, i.e. concentrations relative to the meniscus without having to worry about measuring the offset or meniscus concentration $J(a)$ or $c(a)$ to convert to absolute $J(r)$ or $c(r)$.

## 4
## Polysaccharide Polydispersity and Simple Shape Analysis by Sedimentation Velocity

With sedimentation velocity we measure the change in solute distribution across a solution in an ultracentrifuge cell as a function of time. An example of such a change is given in Fig. 2a for potato amylose [29].

Traditional analysis methods on these measurements have been based around recording the movement of the radial position of the boundary $r_b$ with time $t$, from which a sedimentation coefficient, $s$ (sec or Svedbergs, S, where 1 S = $10^{-13}$ sec) can be obtained (see, e.g. [30]):

$$s = (\mathrm{d}r_b/\mathrm{d}t)/\omega^2 r_b \tag{2}$$

$\omega$ is the angular velocity (rad/$s$) = $(2\pi/60) \times$ rpm. Since the measured $s$ will be affected by the temperature, density and viscosity of the solvent in which it is dissolved it is usual to normalise to standard conditions—namely the density and viscosity of water at 20.0 °C to yield $s_{20,w}$ [30].

$$s_{20,w} = \{(1 - \overline{v}\rho_{20,w})/(1 - \overline{v}\rho_0)\}.\{\eta_0/\eta_{20,w}\}s_{T,b} \tag{3}$$

$\rho_0$ and $\eta_0$ are the densities and viscosities of the solvent, $\rho_{20,w}$ and $\eta_{20,w}$ the corresponding values at 20.0 °C in water. $\overline{v}$ is the partial specific volume, which for neutral polysaccharides can often be reasonably estimated from the carbohydrate content [31] and takes on values between 0.5–0.7 ml/g for

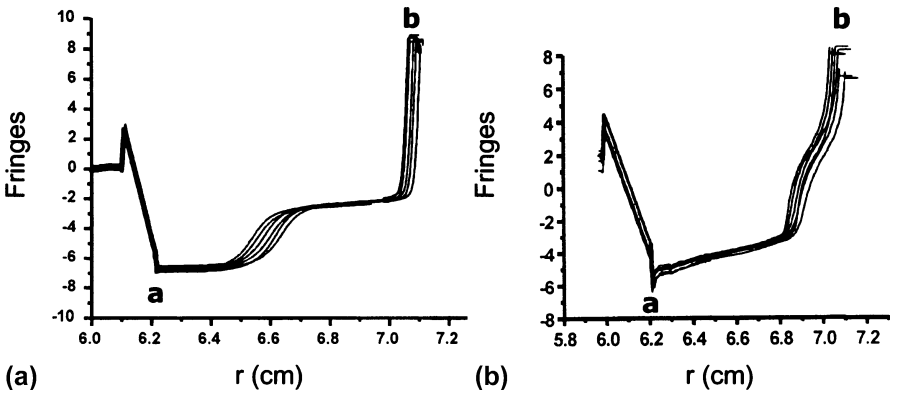


**Fig. 2** Sedimentation velocity diagrams for starch polysaccharides. **a** Sedimenting boundary for potato amylose, scanned at different times. Sample concentration was 8 mg/ml in 90% in dimethyl sulphoxide. Rotor speed was 50 000 rpm at a temperature of 20 °C. **b** Sedimenting boundary for wheat starch (containing amylose and the faster moving amylopectin), scanned at different times. Total sample concentration was 8 mg/ml in 90% in dimethyl sulphoxide. Rotor speed was 35 000 rpm at a temperature of 20 °C. The direction of sedimentation in both **a** and **b** is from left to right. From [29]

neutral polysaccharides in aqueous solvent. In cases where estimates based on composition cannot be reasonably made—such as for polyanionic and polycationic materials—$\overline{v}$ can be measured by densimetry [32] coupled with an accurate concentration measurement. For example Preston and Wik [28] have shown that $\overline{v}$ varies from 0.47 to 0.57 from ionic strengths 0.001 to 0.25 mol $L^{-1}$ (see Table 3).

A computer algorithm SEDNTERP [33, 34] has been developed for facilitating the correction in Eq. 3. There is no longer any need (except for unusual solvents) to look up solvent densities and viscosities in the Chemical Rubber Handbook or other data books—a user of the algorithm just has to specify the buffer composition and the temperature of the measurement and the correction is done automatically.

The $s$ and $s_{20,w}$ obtained from Eqs. 1–3 will be *apparent* values because of the effects of solution non-ideality, deriving from co-exclusion and—for charged polysaccharides—polyelectrolyte effects [30]. To eliminate the effects of non-ideality it is necessary to measure either $s$ or $s_{20,w}$ for a range of different cell loading concentrations $c$, and perform an extrapolation to zero concentration. For polysaccharides this has been conventionally achieved from a plot of $1/s$ (or $1/s_{20,w}$) versus $c$ [30]:

$$\{1/s\} = \{1/s^0\} \cdot \{1 + k_s c\} \tag{4}$$

a relation valid over a limited range of concentration. $k_s$ is the Gralén coefficient named after Svedberg's doctoral student who introduced this term in his 1944 thesis on the analysis of cellulose and its derivatives [35].

For a wider span of concentrations, a more comprehensive description of concentration dependence has been given by Rowe [36, 37]:

$$s = s^0 \left\{1 - \left[k_s c - \left(\left((c v_s)^2 (2\phi_p - 1)\right) / \phi_p^2\right)\right] / [k_s c - 2 c v_s + 1]\right\} \tag{5}$$

$v_s$ (ml/g) is the "swollen" specific volume of the solute [volume (ml) of a polysaccharide swollen though solvent association per gram of the anhydrous molecule] and $\phi_p$ is the maximum packing fraction of the solute ($\sim 0.4$ for biological solutes [37]). A least-squares proFit (Quantum Soft, Zurich, Switzerland) algorithm has been developed for fitting $s$ vs. $c$ data to Eq. 5 and examples of fitting this relation to wheat starch amylose and amylopectin are given in Fig. 3 [29].

For a polydisperse solution—the hallmark of solutions of polysaccharides—$s$ (and $s^0$) will be a weight average [30, 38, 39]. If the solution contains more than one discrete (macromolecular) species—e.g. a mixture of different polysaccharides, the polydispersity will be manifested by asymmetry in the sedimenting boundary or, if the species have significantly different values for $s_{20,w}$, discrete boundaries are resolved (Fig. 2b [29]).

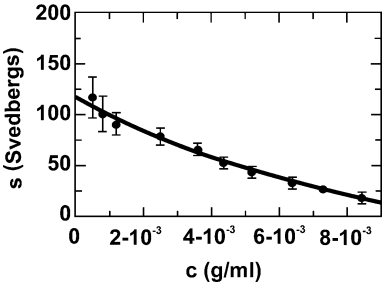


**Fig. 3** Concentration dependence of the sedimentation coefficient for wheat amylopectin. The data have been fitted to Eq. 5 (see text) yielding $s^0 = (120 \pm 10)S$, $k_s = (170 \pm 60)$ml/g and $\nu_s = (40 \pm 4)$ml/g. From [29]

## 4.1
## Sedimentation Coefficient Distributions: DCDT and SEDFIT

Since the appearance of the new generation analytical ultracentrifuges in 1990 (XL-A) and 1996 (XL-I), the acquisition of multiple on-line data acquisition has resulted in some important advances in the software for recording and analysing not only the change in boundary position with time but the change in the whole radial concentration profile, $c(r, t)$ with time $t$. This advance has in particular facilitated the measurement of *distributions* of sedimentation coefficient [40–43]. The (differential) distribution of sedimentation coefficients $g(s)$ can be defined as the population (weight fraction) of species with a sedimentation coefficient between $s$ and $s + ds$ [40]. A plot of $g(s)$ versus $s$ then defines the distribution. Integration of a peak or resolved peaks of a $g(s)$ vs. $s$ plot can then be used to calculate the weight average $s$ of the sedimenting species and their partial loading concentrations.

## 4.2
## Time Derivative Analysis: DCDT

The simplest way computationally of obtaining a sedimentation coefficient distribution is from time derivative analysis of the evolving concentration distribution profile across the cell [40, 41]. The time derivative at each radial position $r$ is $(\partial\{c(r,t)/c_0\}/\partial t)_r$ where $c_0$ is the initial loading concentration. Assuming that a sufficiently small time integral of scans are chosen so that $\Delta c(r,t)/\Delta t = \partial c(r,t)/\partial t$ the apparent weight fraction distribution function $g^*(s)$ {n.b. sometimes written as $g(s^*)$} can be calculated

$$g^*(s) = \{\partial\{c(r,t)/c_0\}/\partial t\} \cdot \left\{(\omega^2 t^2)/\ln(a/r)\right\} \cdot \{(r/a)^2\} \tag{6}$$

and the abscissa

$$s = \{\ln(a/r)\} \cdot 1/\{\omega^2 t\} \tag{7}$$

where $a$ is the radial position of the meniscus. In this way the evolving $c(r, t)$ versus $r$ profiles are transformed into an apparent sedimentation coefficient distribution plot. The asterisk is used to indicate that the distributions calculated using this equation are "apparent" in the sense they are not corrected for diffusion effects (nor, as is often forgotten, non-ideality). Depending on how fast the diffusion process is (for large polysaccharides this can be small compared to the sedimentation process) this will cause an overestimate of the width of a sedimentation coefficient distribution, but not on the weight average sedimentation coefficient. This procedure forms the basis of the *DCDT* algorithm developed by W. Stafford [40] later refined by J. Philo as *DCDT+* [41, 44]. The success of the method depends on data sampling at high frequency and a large spectrum of radial positions so as to reduce random noise. It has the great facility that time independent noise is eliminated in the differential.

Figure 4 [29] shows the $g^*(s)$ versus profiles for potato amylose and the amylose/amylopectin mixture from wheat starch corresponding to the concentration versus radial displacement data of Fig. 3. The $s$ data used in the concentration dependence plot of Fig. 3 for wheat amylopectin comes from $g^*(s)$ vs. $s$ analysis data of Fig. 2b and similar. The concentrations shown in the abscissa in Fig. 4 have been obtained from the total starch loading concentration normalised by the weight fraction of the amylopectin component estimated from the $g^*(s)$ vs. $s$ profiles.

Various improvements of the DCDT [40, 41] approach have been considered to correct for the effects of diffusion, based largely around extrapolation to $(1/\sqrt{t}) \rightarrow 0$.

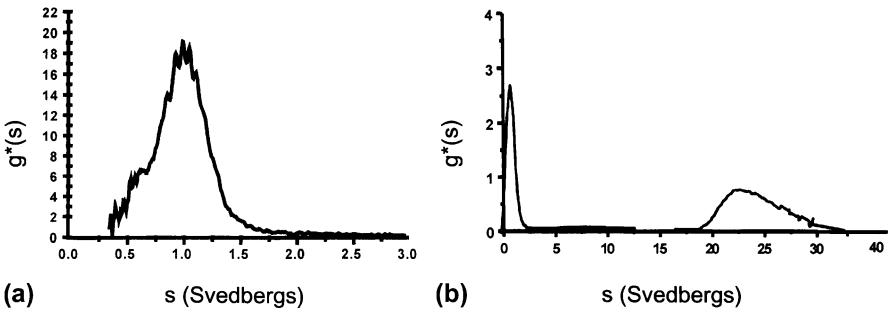


**Fig. 4** Sedimentation velocity $g^*(s)$ profiles for starch polysaccharides using DCDT+. The profiles correspond to the radial displacement plots of Fig. 2. **a** Potato amylose, sample concentration 8 mg/ml in 90% in dimethyl sulphoxide. Rotor speed was 50 000 rpm at a temperature of 20 °C. **b** Wheat starch (containing amylose, left peak and the faster moving amylopectin, right peak), (total) sample concentration 8 mg/ml in 90% dimethyl sulphoxide. Rotor speed was 35 000 rpm at a temperature of 20 °C. From [29]

### 4.3 Lamm Equation Approach: SEDFIT

More recently, attention has turned to direct modelling of the evolution of the concentration distribution with time for obtaining the sedimentation coefficient distribution. The notation used in this approach is a little different [42, 43], $c(s)$ being chosen to represent the (differential) distribution of sedimentation coefficients (not as $g(s)$ previous [30, 40, 41]) although it is still defined as the population of species with a sedimentation coefficient between $s$ and $s + \mathrm{d}s$. Despite the perhaps confusing use of the symbol $c(s)$ it does not have the units of weight concentration, but weight concentration per sedimentation coefficient (e.g. $\mathrm{g.ml^{-1}.S^{-1}}$). The distribution has been related to the experimentally measured evolution of the concentration profiles throughout the cell by a Fredholm integral equation

$$a(r,t) = \int_{s_{\min}}^{s_{\max}} c(s) \cdot \chi(s, D, r, t)\,\mathrm{d}s + a_{\mathrm{TI}}(r) + a_{\mathrm{RI}}(t) + \varepsilon \tag{8}$$

In this relation $a(r,t)$ is the experimentally observed signal, $\varepsilon$ represents random noise, $a_{\mathrm{TI}}(r)$ represents the time invariant systematic noise and $a_{\mathrm{RI}}(t)$ the radial invariant systematic noise: Schuck [42] and Dam and Schuck [43] describe how this systematic noise is eliminated. $\chi$ is the normalised concentration at $r$ and $t$ for a given sedimenting species of sedimentation coefficient $s$ and translational diffusion coefficient $D$: it is normalised to the initial loading concentration so it is dimensionless.

The evolution with time of the concentration profile $\chi(s, D, r, t)$ in a sector shaped ultracentrifuge cell is given by the Lamm [45] equation:

$$\frac{\partial \chi}{\partial t} = (1/r) \cdot \frac{\partial}{\partial r}\left[ rD\frac{\partial \chi}{\partial r} - s\omega^2 r^2 \chi \right] \tag{9}$$

Although only approximate analytical solutions to this partial differential equation have been available for $\chi(s, D, r, t)$, accurate numerical solutions are now possible using finite element methods first introduced by Claverie and coworkers [46] and recently generalized to permit greater efficiency and stability [42, 43]: the algorithm SEDFIT [47] employs this procedure for obtaining the sedimentation coefficient distribution.

To solve Eq. 8 to obtain $c(s)$ as a function of $s$ requires $s_{\min}$ and $s_{\max}$ to be carefully chosen and adjusted accordingly: inappropriate choice can be diagnosed by an increase of $c(s)$ towards the limits of $s_{\min}$ or $s_{\max}$. However, a stable solution can only be obtained if the contribution from diffusion broadening is dealt with.

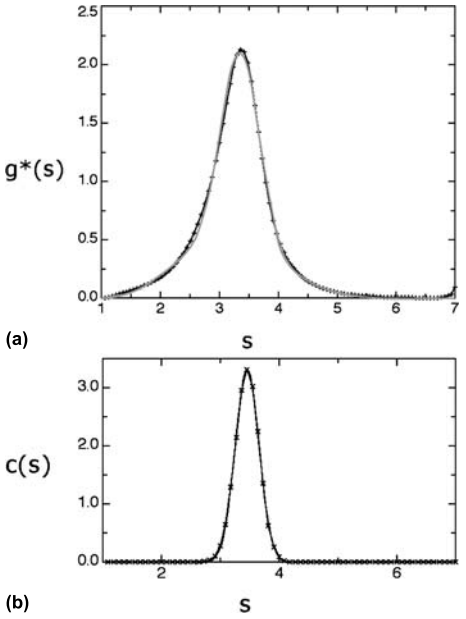


**Fig. 5** Sedimentation concentration distribution plots for guar gum using SEDFIT. **a** $g^*(s)$ vs. $s$ **b** $c(s)$ vs. $s$. A Gaussian fit to the data (*lighter line*) is also shown in (**a**). Rotor speed was 40 000 rpm at 20.0 °C, concentration was 0.75 mg/ml in 0.02% $NaN_3$. The guar had been heated at 160 °C for 10 min at a pressure of 3 bar. From [49]

SEDFIT tries to do this by using a dependence of $D$ on $s$, and it does so by making use of a link involving the translational frictional ratio $f/f_0$:

$$D(s) = \left\{\left(\sqrt{2}\right)/(18\pi)\right\} \cdot k_B t \cdot s^{-1/2} \left(\eta_0 (f/f_0)_w\right)^{-3/2} \left((1 - \overline{v}\rho_0)/\overline{v}\right)^{-1/2} \qquad (10)$$

$f$ is the frictional coefficient of a species and $f_0$ the corresponding value for a spherical particle of the same mass and (anhydrous) volume (see e.g. [48]). $k_B$ is the Boltzmann constant. Although of course a distribution of $s$ implies also a distribution in $D$ and $f/f_0$, for protein work advantage is taken of the fact that the frictional ratio is a relatively insensitive function of concentration: a single or weight average $f/f_0$ is taken to be representative of the distribution. It is open to question for large linear macromolecules like many polysaccharides. If this assumption is valid Eq. 8 can be numerically inverted—i.e. solved—to give the sedimentation coefficient distribution, with the position and shape of the $c(s)$ peak(s) more representative of a true distribution of sedimentation coefficient. $(f/f_0)_w$, where the subscript $w$ denotes a weight average, is determined iteratively by non-linear regression, optimizing the quality of the fit of the $c(s)$ as a function of $(f/f_0)_w$. It has been shown by extensive simulation that non-optimal values of $(f/f_0)_w$ have little effect on the position of the $c(s)$ peaks, although effect the

width and resolution, i.e. the correct $s$ value is reported. Regularization [47] can be used which provides a measure of the quality of fit from the data analysis.

SEDFIT also offers the option of evaluating the distribution corresponding to non-diffusing particles, viz $D \sim 0$, i.e. the diffusive contribution to Eq. 8 is small compared to the sedimentation contribution. In this case Eq. 8 can be inverted without any assumptions concerning $f/f_0$. If diffusive affects are significant it will be an apparent sedimentation coefficient distribution, i.e. $g^*(s)$ vs. $s$, analogous to that produced by the DCDT procedure, and the correct $s$ value for a peak is still reported. This procedure, called the "least squares" $g^*(s)$ procedure to distinguish it from DCDT has the advantage over DCDT in that errors caused by the approximation $\Delta t \sim \mathrm{d}t$ are absent. Figure 5 gives a comparison of the least squares $g^*(s)$ vs. $s$ and $c(s)$ vs. $s$ distribution for guar gum [49]. Least squares $g^*(s)$ vs. $s$ is currently our method of choice for polysaccharides.

### 4.4
### Molecular Weight and Conformation

The sedimentation coefficient $s^0$, or its normalized form $s^0_{20,w}$ is a function of the conformation and flexibility of a macromolecule (via its translational frictional property) and its mass. So if we are going to obtain conformation and flexibility information we need to know the molecular weight (molar mass) and *vice verse*.

It is possible to get molecular weight from the sedimentation coefficient if we assume a conformation or if we combine with other measurements, namely the translational diffusion coefficient via the Svedberg equation [50]

$$M = RT \cdot \{s^0/D^0\}/(1 - \overline{v}\rho_0) \tag{11}$$

where $\rho_0$ is the solvent density (if $s$ and $D$ are their normalized values $s^0_{20,w}$, $D^0_{20,w}$, $\rho_0$ will be the density of water at 20.0 °C, 0.9981 g/ml).

Equation 11 has been popularly used for example to investigate the molecular weights of carboxymethylchitins [51–53], glycodendrimers [54, 55], galactomannans [56], beta-glucans [57, 58] and alginates [59].

The translational diffusion coefficient in Eq. 11 can in principle be measured from boundary spreading as manifested for example in the width of the $g^*(s)$ profiles: although for monodisperse proteins this works well, for polysaccharides interpretation is seriously complicated by broadening through polydispersity. Instead special cells can be used which allow for the formation of an artificial boundary whose diffusion can be recorded with time at low speed ($\sim$ 3000 rev/min). This procedure has been successfully employed for example in a recent study on heparin fractions [5]. Dynamic light scattering has been used as a popular alternative, and a good demonstra-

tion of how this can be performed to give reliable $D$ data has been given by Burchard [3].

Whereas the $s^0$ is a weight average, the value returned from dynamic light scattering for $D^0$ is a $z$-average. As shown by Pusey [60] combination of the two via the Svedberg Eq. 11 yields the weight average molecular weight, $M_w$, although it is not clear what type of average for $M$ is returned if an estimate for $D^0$ is made from ultracentrifuge measurements.

Another useful combination that has been suggested is $s^0_{20,w}$ with $k_s$ [36, 37]

$$M_w = N_A \left[6\pi\eta s^0_{20,w}/(1 - \overline{v}\rho_0)\right]^{3/2} [(3\overline{v}/4\pi)(k_s/2\overline{v}) - (\nu_s/\overline{v})]^{1/2} \quad (12)$$

$s$, $k_s$ and $\nu_s$ can be obtained from fitting $s$ vs. $c$ data to Eq. 5. The method was originally developed for single solutes and where charge effects can be neglected (either because the macromolecular solute is uncharged, or because the double layer or polyelectrolyte behaviour has been "compressed" by addition of neutral salt). For quasi-continuous distributions, such as polysaccharides one can apply Eqs. 5 and 12 to the data, provided that for every concentration one has a "boundary" to which a weight-averaged $s$ value can be assigned. If the plot of $1/s$ vs. $c$ is essentially linear over the data range, then specific interaction can be excluded, the solute system treated as a simple mixture and Eqs. 5 and 12 can be applied.

For wheat starch amylopectin for example (cf. Fig. 3) a value for $M_w$ of $\sim 30 \times 10^6$ g/mol is estimated [29]. This equation is only approximate—any contributions from molecular charge to the concentration dependence parameter $k_s$ are assumed to be negligible or suppressed—but is nonetheless very useful when other methods—especially for very large polysaccharides like amylopectin—are inapplicable. The method also yields an estimate for the swollen specific volume $\nu_s$: for example Majzoobi has obtained a value of $(40 \pm 4)$ ml/g for wheat starch amylopectin [29]. For polydisperse materials such as polysaccharides the question is what sort of average $M$ value is yielded by this method? In the absence of any obvious analytical solution, computer simulation has been used to determine the form of the average. In work to be published, A.J. Rowe and coworkers have shown that even for "unfavourable" simulated mixtures (e.g. multi-modal, no central tendency), the average $M$ value yielded is very close to an $M_w$ (i.e. weight-averaged $M$). To put this in quantitative terms, the departure from $M_w$ is generally < 1% of the way towards $M_z$. This is trivial, in terms of the errors present in the raw data. Thus, there is an exact procedure which can be defined for the evaluation of $M$(average) in a polydisperse solute system under the defined conditions, and simulation demonstrates that for all practical purposes the outcome is an $M_w$.

A sedimentation coefficient *distribution*—either $c(s)$ versus $s$ or $g^*(s)$ vs. $s$—for a polysaccharide can also be converted into an apparent molecular weight distribution if the conformation of the polysaccharide is known or can

be assumed, via a power law or "scaling" relation:

$$s^0 = K'' M^b \tag{13}$$

where the power law exponent is dependent on the conformation of the macromolecule, with the limits, in the case of non-draining molecules $b \sim 0.15$ for a rigid rod and $\sim 0.67$ for a compact sphere. A flexible coil shape molecule has a $b \sim 0.4 - 0.5$ [61, 62]. An early example of this transformation has been given for a heavily glycosylated mucin glycoprotein with polysaccharide like properties [63] based on a $g^*(s)$ vs. $s$ distribution given by Pain [64]). The assumption was made that the contribution from diffusion broadening of these large molecules was negligible in comparison to sedimentation. Incorporation of Eq. 13 instead of Eq. 10 into the $c(s)$ vs. $s$ evaluation process is now being considered for polysaccharides.

Conversely, if we know the molecular weight we can make inferences about the conformation of polysaccharides in solution using Eq. 13 and other power-law relations. We will consider this in more detail after we have considered further molecular weight measurement by absolute (i.e. without assumptions concerning conformation) procedures.

## 5 Polysaccharide Molecular Weight Analysis by Sedimentation Equilibrium

Whereas in a sedimentation velocity experiment at relatively high rotor speed—for a polysaccharide say 40 000–50 000 rev/min—the sedimentation rate and hence sedimentation coefficient are a measure of the size and shape of the molecule, at much lower speeds, say 10 000 rev/min or less in a sedimentation equilibrium experiment, the forces of sedimentation and diffusion on the macromolecule become comparable and instead of producing a sedimenting boundary a steady state equilibrium distribution of macromolecule is attained with a low concentration at the air/solution meniscus building up to a high concentration at the cell base. This final steady state pattern [65] is a function only of molecular weight and related parameters (non-ideal virial coefficients and association constants were appropriate) and not on molecular shape since at equilibrium there is no net transport or frictional effects: sedimentation equilibrium in the analytical ultracentrifuge is an absolute way of estimating molecular weight.

## 5.1
## Molecular Weight Information Obtained

Since polysaccharides are by their very nature polydisperse, the value obtained will be an average of some sort. With Rayleigh interference and, where appropriate, UV-absorption optics, the principal average obtained is the weight average, $M_w$ [30]. Although relations are available for obtaining also number average $M_n$ and $z$-average $M_z$ data these latter averages are difficult to obtain with any reliable precision. Direct recording of the concentration gradient $dc/dr$ versus radial displacement $r$ using refractive index gradient or "Schlieren" optics however facilitates the measurement of $M_z$ (see [66]). Such an optical system is unfortunately not present on the present generation XL-A or XL-I ultracentrifuges except for in-house adapted preparative XL ultracentrifuges [67]. Schlieren optics are also present on the older generation Model E analytical ultracentrifuge: this is one of the main reasons why we at the NCMH keep and maintain one of these instruments [68].

An important consideration with polysaccharides is that at sedimentation equilibrium there will be a redistribution not only of total concentration of polysaccharide throughout the cell (low concentration at the meniscus building up to a higher concentration at the cell base) but also a redistribution of species of different molecular weight, with a greater proportion of the higher molecular weight part of the distribution appearing near the cell base. In obtaining a true weight (or number, $z$ averages) it is therefore important to consider the *complete* concentration distribution profile throughout the ultracentrifuge cell. As with our description of sedimentation velocity, for clarity we will confine our consideration only to the extraction of the two most directly related parameters: the weight average molecular weight and the molecular weight distribution. The extraction of other parameters—such as point average data—are avoided here but can be found in other articles (see [9, 11, 69, 70]).

## 5.2
## Obtaining the Weight Average Molecular Weight: MSTAR

As stated above UV-absorption optics – when they can be applied – have the advantage that the recorded absorbances $A(r)$ as a function of radial position are (within the Lambert–Beer law limit of $A(r) \sim 1.4$) directly proportional to the weight concentration $c(r)$ in g/ml. Although the multiple fringes in interference optics give a much more precise record of concentration, we stress again, these are *concentrations relative to the meniscus*. That is we obtain directly from the optical records a profile of $c(r) - c(a)$ versus radial displacement $r$, with the meniscus at $r = a$. In fringe displacement units this is $J(r) - J(a)$, which we write as $j(r)$ for short. To obtain molecular weight information we need $J(r)$ and hence some way of obtaining $J(a)$ is required: this is not

such a requirement for sedimentation velocity where relative concentrations are sufficient. At this stage it is worth pointing out there are three types of sedimentation equilibrium experiment which depend on the conditions used (namely speed and solution column length in the centrifuge cell):

(i) the low speed method [71] in which the solute (polysaccharide) concentration at the meniscus {$c(a)$ or, in fringe displacement units, $J(a)$} remains finite,
(ii) the high speed or "meniscus depletion" method [72] in which the concentration at the meniscus is effectively zero,
(iii) the intermediate speed method [73] in which the solute concentration at the meniscus remains small but finite.

Extraction of molecular weight data from the optical records is considerably easier for the meniscus depletion method since no estimate for $J(a)$ is required. This procedure has in the past been popular for protein work because it not only avoids the problem of $J(a)$ measurement but also facilitates the evaluation of number average molecular weight data. Sadly, this is not generally applicable to solutions of polysaccharides because of their polydispersity: at sedimentation equilibrium a polydisperse solution will tend to redistribute its species so there is a greater proportion of higher molecular weight species near the cell base. Any attempt to deplete the meniscus (rich in the lower molecular weight part of the distribution) of polysaccharide is almost guaranteed to result in loss of optical registration of the interference fringes near the bottom of the cell, leading to underestimates for $M$. A further difficulty in attempting to achieve meniscus depletion conditions is that the effective thermodynamic non-ideality of the system—which can also lead to an underestimate for $M$—is increased at higher rotor speed: this is discussed later in this article.

So methods (i) or (iii) are required. Further, since the greater the difference between the concentration at the meniscus $J(a)$ and the cell base $J(b)$ the smaller will be the effect of errors in $J(a)$ on the final molecular weight evaluated, for polysaccharides the intermediate speed method, (iii) should be the method of choice. This means that a procedure for evaluating $J(a)$ is required. It was recently shown by Hall and coworkers [74] that simply floating it as another variable in the procedure for extracting $M$ is not valid, particularly for polydisperse or interacting systems. A convenient procedure for extracting $J(a)$ and then $M$ was given by Creeth and Harding in 1982 [73], and is briefly summarised now.

The fundamental equation of sedimentation equilibrium can be manipulated to define a new function with dimensions of molar mass (g/mol) called $M^*(r)$. $M^*(r)$ at a radial position $r$ is defined by

$$M^*(r) = \frac{j(r)}{\left\{kJ(a)\left(r^2 - a^2\right) + 2k\int_a^r r \cdot j(r)\,\mathrm{d}r\right\}} \tag{14}$$

where $k = (1 - \overline{v}\rho_0)\omega^2/2RT$, with $\rho_0$ the solvent density. Equation 14 has the limiting form

$$\lim_{r \to a} \left\{ j(r) / \left( r^2 - a^2 \right) \right\} = k \cdot M^*(a) \cdot J(a) \,. \tag{15}$$

A plot of $j(r)/(r^2 - a^2)$ vs. $\{1/(r^2 - a^2)\} \cdot \int_a^r r \cdot j(r) \mathrm{d}r$ therefore has a limiting slope of $2kM^*(a)$ and an intercept $kM^*(a).J(a)$. Hence $J(a)$ is determinable from $2 \times$ (intercept/limiting slope).

It is worth pointing out that Teller and coworkers [75] have considered other manipulations involving representations similar to Eqs. 14 and 15 for obtaining $J(a)$. Other methods of obtaining $J(a)$ have been considered in detail by Creeth and Pain [76]. More recently Minton [77] has given an almost identical procedure, although he appears to have missed the original Creeth and Harding article published 12 years previous [73]. Once $J(a)$ has been found $M^*$ as a function of radial position $r$ can be defined.

A particularly useful property of the $M^*$ function is that at the cell base ($r = b$),

$$M^*(b) = M_{\mathrm{w,app}} \tag{16}$$

the apparent weight average molecular weight of the polysaccharide [73]. It will be an apparent value because it will be affected by thermodynamic non-ideality (molecular co-exclusion and, for charged polysaccharides, polyelectrolyte behaviour), which needs to be corrected for (see below). The $M^*$ procedure for obtaining $M_{\mathrm{w,app}}$ can be thought of in terms of the "*PACMAN*" computer game: $M^*(r)$ becomes closer and closer to $M_{\mathrm{w,app}}$ as the integral consumes more and more data as the cell base is approached ($r \to b$). Optical distortion effects at the cell base means that a short extrapolation of $M^*(r)$ to $M^*(= b)$ is required, but this normally poses no difficulty. An example is given in Fig. 6. Practical details behind the MSTAR algorithm [78] upon which this procedure is based can be found in [69].

It is worth pointing out here that another popular algorithm for analysing molecular weight from sedimentation equilibrium is *NONLIN* [79]. Whereas this is useful for the analysis of protein systems (monodisperse or associating), for a polydisperse system like polysaccharides it is unsuitable: the estimate for $M_{\mathrm{w,app}}$ obtained refers to only to a selected region of the ultracentrifuge cell, and provides no rigorous procedure for dealing with the meniscus concentration problem.

One can see the $M^*$ procedure has a parallel to either $g^*(s)$ vs. $s$ or $c(s)$ vs. $s$ in sedimentation velocity where the data are transformed from radial displacement space [concentration, $c(r)$ versus $r$] to sedimentation coefficient space [$g^*(s)$ or $c(s)$ versus $s$]. Here we are transforming the data from concentration space [concentration relative to the meniscus $j(r)$ versus $r$] to molecular weight space [$M^*(r)$ versus $r$].

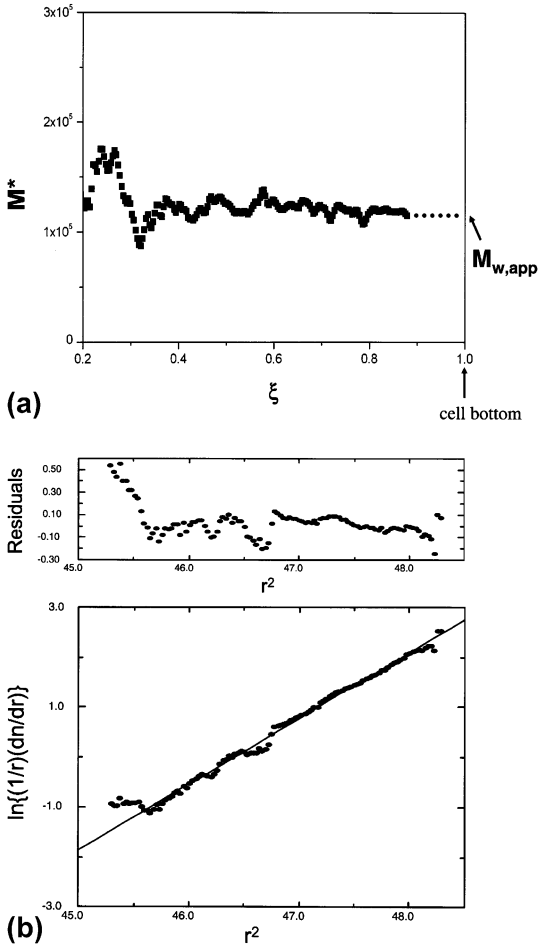


**Fig. 6** Sedimentation equilibrium of chitosans **a** MSTAR analysis for $M_{w,app}$, from optical registration of the concentration distribution using Rayleigh interference optics on the XL-I ultracentrifuge and Eqs. 14 and 15 (see text) for chitosan G213. $M_{w,app}$ = 110 000 g/mol. $\xi$, is a normalised radial displacement squared parameter: $\xi = (r^2 - a^2)/(b^2 - a^2)$ where $r$ is the radial displacement from the axis of rotation at a given point in the ultracentrifuge cell, and $a$ and $b$ the corresponding radial positions at the solution meniscus and cell base respectively. $\xi = 0$ at the meniscus and = 1 at the cell base. Loading concentration 1.0 mg/ml in 0.2 M acetate buffer. **b** Analysis for $M_{z,app}$ using optical registration of the concentration gradient distribution using the Schlieren optics on the Model E ultracentrifuge for chitosan G214 at 0.3 mg/ml in 0.2 M acetate buffer. The line fitted is to $\ln\{(1/r)(\mathrm{d}n/\mathrm{d}r)\} = \{M_{z,app}(1 - \overline{v}\rho_0)\omega^2/2RT\}r^2$. $M_{z,app}$ = 215 000 g/mol. Rotor speed = 10 000 rpm. From [144]

## 5.3 Correcting for Thermodynamic Non-Ideality: Obtaining $M_w$ from $M_{w,app}$

For polysaccharides, non-ideality arising from co-exclusion volume and polyelectrolyte effects, can be a serious problem (Table 4), and, if not corrected for, can lead to significant underestimates for $M_w$. It was possible with the older generation Model E ultracentrifuges—which could accommodate long (30 mm) optical path length cells—to work at very low solute loading concentrations (0.2 mg/ml). At these concentrations for some polysaccharides—particularly neutral ones or those of molecular weight < 100 000 g/mol—the non-ideality effect could be neglected: the estimate for $M_{w,app}$ was within a few percent of the true or "ideal" $M_w$. However, the new generation XL-I can only accommodate a maximum 12 mm optical path length cell with a minimum concentration requirement of 0.5 mg/ml: lower concentrations produce insufficient fringe displacement for meaningful analysis. This is another reason why we have kept running a Model E ultracentrifuge in the NCMH: the ability to use the longer path length cells makes a large difference to the severity of the non-ideality problem as Table 4 [80–88] shows. The term $(1 + 2BM_wc)$, where $B$ is the thermodynamic second virial coefficient, represents the factor by which the apparent molecular weight measured at a finite concentration $c = 0.2$ mg/ml and 0.5 mg/ml underestimates the true or ideal $M_w$. One can see that whereas the earlier lower limit (0.2 mg/ml) for many

**Table 4** Comparative non-ideality of polysaccharides

| | $10^{-6} \times M$ (g mol$^{-1}$) | $10^4 \times B$ (ml mol g$^{-2}$) | $BM$ (ml/g) | $1 + 2BMc$[a] | $1 + 2BMc$[b] | Ref. |
|---|---|---|---|---|---|---|
| Pullulan P5 | 0.0053 | 10.3 | 5.5 | 1.002 | 1.006 | [80] |
| Pullulan P50 | 0.047 | 5.5 | 25.9 | 1.010 | 1.026 | [80] |
| Xanthan (fraction) | 0.36 | 2.4 | 86 | 1.035 | 1.086 | [81] |
| $\beta$-glucan | 0.17 | 6.1 | 104 | 1.042 | 1.104 | [82] |
| Dextran T-500 | 0.42 | 3.4 | 143 | 1.057 | 1.143 | [83] |
| Pullulan P800 | 0.76 | 2.3 | 175 | 1.070 | 1.175 | [80] |
| Chitosan (Protan 203) | 0.44 | 5.1 | 224 | 1.090 | 1.224 | [84] |
| Pullulan P1200 | 1.24 | 2.2 | 273 | 1.109 | 1.273 | [80] |
| Pectin (citrus fraction) | 0.045 | 50.0 | 450 | 1.180 | 1.450 | [85] |
| Scleroglucan | 5.7 | 0.50 | 570 | 1.228 | 1.570 | [86, 87] |
| Alginate | 0.35 | 29.0 | 1015 | 1.406 | 2.015 | [88, 91] |

[a] Based on a loading concentration of 0.2 mg/ml.
[b] Based on a loading concentration of 0.5 mg/ml.

cases led to only small errors, with the new instruments (limit 0.5 mg/ml) leading to severe underestimates in virtually all cases.

For polyelectrolytes the second virial coefficient is very sensitive to ionic strength. Preston and Wik [28] have shown a tenfold increase in $B$—from $\sim$ 50 ml mol g$^{-2}$ to $\sim$ 500 ml mol g$^{-2}$—upon decreasing the ionic strength from 0.2 down to 0.01 mol l$^{-1}$.

However, it is usually easy, if a little laborious, to correct for non-ideality. Measurement of $M_{w,app}$ over a range of loading concentrations is necessary followed by an extrapolation to zero concentration using an equation of the form [76]

$$\{1/M_{w,app}\} = \{1/M_w\} + 2Bc$$
$$= \{1/M_w\}(1 + 2BM_w c) \quad (17)$$

correct to first order in concentration. The availability of four and eight-hole rotors in the XL-A and XL-I means that several concentrations can be run simultaneously. Further multiplexing is possible with the use of phantis-style 6-channel ultracentrifuge cells [72], which permit the simultaneous measurement of three solution/reference solvent pairs, although these tend to return $M_{w,app}$ values of lower accuracy. Figure 7 shows an example for xanthan [90].

The second virial coefficient $B$ in Eq. 17 refers to the static case. In the ultracentrifuge the measured value can show a speed dependence [39], an effect which can be minimized by using low speeds and short solution columns. If present it will not affect the value of $M_w$ after extrapolation to zero concentration.

In some extreme cases, third or even higher virial coefficient(s) may be necessary to adequately represent the data: for example $\kappa$-carrageenan [90] and alginate [91]. In a further study on alginates, Straatman and Borchard [92] demonstrated excellent agreement between $M_w$ and $B$ values ob-

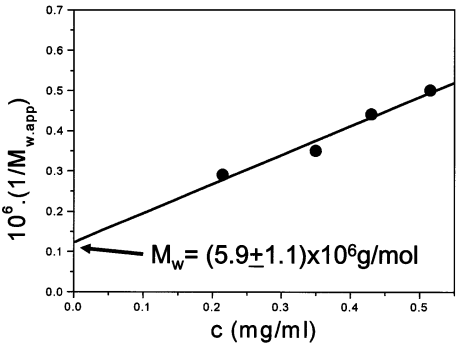


**Fig. 7** Concentration extrapolation of $1/M_{w,app}$ to obtain $M_w$ for xanthan. Rotor speed = 3000 rpm. Phosphate chloride buffer (pH = 6.5, $I$ = 0.3). From [89]

tained from sedimentation equilibrium and light scattering methods. Preston and Wik [28] have shown for a different polyelectrolyte—hyaluronan—how increasing the ionic strength can keep $B$ to a minimum.

## 5.4 Distributions of Molecular Weight

Direct inversions of the concentration distribution profiles to obtain molecular weight distribution information are generally impossible because of complications involving non-ideality. Successful attempts have been given but only for simple discrete forms of polydispersity (two to three macromolecular species [93]).

The simplest procedure for avoiding these complications [94] is to use sedimentation equilibrium in conjunction with gel permeation chromatography (GPC). Fractions of relatively narrow (elution volume) band width are isolated from the eluate and their $M_w$ values evaluated by low speed sedimentation equilibrium in the usual way: the GPC columns can thereby be "self-calibrated" and elution volume values converted into corresponding molecular weights—a distribution can therefore be defined in a way which avoids the problem of using inappropriate standards for GPC: the value of multiplexing is clearly indicated. This procedure has been successfully applied to for example dextrans, alginates and pectins: for pectins excellent agreement with analogous procedures involving classical light scattering coupled to GPC has been obtained [95].

## 5.5 Number and $z$-Averages: Polydispersity Index

Molecular weights of polysaccharides in solution can also be measured by osmotic pressure and light scattering. Osmotic pressure yields the number average molecular weight, which can be usefully used with $M_w$ from sedimentation equilibrium as a measure of polydispersity: Preston and Wik [28] have done this for example with hyaluronic acid. The ratio $M_w/M_n$ the "polydispersity index" is often given as a measure of polydispersity, and can be related to the width of a molecular weight distribution via the well-known Herdan [96] relation:

$$\{\sigma_n/M_n\} = [(M_w/M_n) - 1]^{1/2} \tag{18}$$

where $\sigma_n$ is the number-average standard deviation of the distribution, whatever form it may take. The problem with osmotic pressure is that since the sensitivity depends on the number as opposed to weight concentrations of solute, for polysaccharides of $M_n > 100\,000$ it becomes difficult to apply [97]. An alternative strategy is to measure the $z$-average molecular weight from sedimentation equilibrium using the Schlieren optical system, which records the

concentration gradient (in the form of the refractive index gradient $\mathrm{d}n/\mathrm{d}r$) as a function of radial position $r$, rather than Rayleigh Interference [66]: once again it is a pity that the modern XL-I analytical ultracentrifuge currently does not have this facility. Figure 6b shows a determination of the $M_{z,\mathrm{app}}$ from the slope of a plot of $\ln\{(1/r)(\mathrm{d}n/\mathrm{d}r)\}$ versus $r^2$ for a chitosan under the same solvent conditions as Fig. 6a. Like $M_{\mathrm{w,app}}$, $M_{z,\mathrm{app}}$ has to be corrected for non-ideality. The form of the extrapolation (correct to first order in $c$) is [77]

$$\begin{aligned}\{1/M_{z,\mathrm{app}}\} &= \{1/M_z\} + 4Bc \\ &= \{1/M_z\}(1 + 4BM_z c)\,. \end{aligned} \tag{19}$$

Once $M_z/M_\mathrm{w}$ has been obtained, the corresponding Herdan relation [96] for $M_z/M_\mathrm{w}$ is:

$$\{\sigma_\mathrm{w}/M_\mathrm{w}\} = [(M_z/M_\mathrm{w}) - 1]^{1/2} \tag{20}$$

where $\sigma_\mathrm{w}$ is the weight-average standard deviation of the distribution, whatever form it may take. It is not to be confused with the same symbol unfortunately introduced some 20 years later to represent a reduced weight average molecular weight [98]: use of the original Rinde [99] parameter $A_\mathrm{w}$ for the latter is recommended.

Fujita [38] showed that for a log-normal distribution of molecular weights (the usual case for polysaccharides) $M_z/M_\mathrm{w} \equiv M_\mathrm{w}/M_\mathrm{n}$.

## 5.6 SEC/MALLs and the New Role of Sedimentation Equilibrium

The measurement of the angular dependence of the total intensity of light scattered by solutions of polysaccharides provides, like sedimentation equilibrium, a direct and absolute way of measuring the weight average molecular weight, again if allowance for thermodynamic non-ideality is made (nb. some researchers tend to prefer "$A_2$" as the notation for the 2nd virial coefficient rather than $B$). Although opinions varied, prior to 1990 (see e.g., [100]) there was a good case for suggesting sedimentation equilibrium as the preferred method of choice for the measurement of molecular weights, simply because of the less stringent requirements on sample clarity: with light scattering it is essential that solutions are free of supra-molecular aggregates.

The inclusion of a flow cell into a light scattering photometer facilitated the coupling on-line to a gel permeation chromatography column and SEC-MALLs ("size exclusion chromatography coupled to multi angle laser light scattering") has now revolutionised the measurement of molecular weight and molecular weight distribution [4, 101]. The combined effect of the SEC columns and a pre- or "guard column" can provide clear fractionated samples to the light scattering cell, facilitating not only measurement of $M_\mathrm{w}$ for the whole distribution, but also the distribution itself. Prior ultracentrifugation

of the polysaccharide solution ($\sim 40\,000$ rpm for 30 mins) is still advisable. The first polysaccharide studies were published in 1991 [102–104] and it is now regarded by many as the method of choice for polysaccharide molecular weight determination. Furthermore, the angular dependence of the scattered light facilitates measurement of $R_g$ as a function of elution volume and hence molecular weight: this provides conformation information about the polysaccharide [105].

Nonetheless, uncertainties can sometimes remain particularly if materials have been incompletely clarified or there are problems with the columns (the form of the angular dependence data can usually tell us if things are not well). Sedimentation equilibrium offers a powerful and valuable independent check on the results generated from SEC-MALLs: although it takes a longer time to generate a result, and molecular weight distributions are considerably more difficult to obtain, agreement of $M_w$ from sedimentation equilibrium with $M_w$ from SEC-MALLs gives the researcher increased confidence in some of the other information (molecular weight distribution and $R_g$–$M$ dependence) coming from the latter.

## 6
## Polysaccharide Conformation Analysis

The sedimentation coefficient $s^0$ provides a useful indicator of polysaccharide conformation and flexibility in solution, particularly if the dependence of $s^0$ on $M_w$ is known [62]. There are two levels of approach: (i) a "general" level in which we are delineating between overall conformation types (coil, rod, sphere); (ii) a more detailed representation where we are trying to specify particle aspect ratios in the case of rigid structures or persistence lengths for linear, flexible structures.

### 6.1
### The Wales–van Holde Ratio

The simplest indicator of conformation comes not from $s^0$ but the sedimentation concentration dependence coefficient, $k_s$. Wales and Van Holde [106] were the first to show that the ratio of $k_s$ to the intrinsic viscosity, $[\eta]$ was a measure of particle conformation. It was shown *empirically* by Creeth and Knight [107] that this has a value of $\sim 1.6$ for compact spheres and non-draining coils, and adopted lower values for more extended structures. Rowe [36, 37] subsequently provided a derivation for rigid particles, a derivation later supported by Lavrenko and coworkers [10]. The Rowe theory assumed there were no free-draining effects and also that the solvent had suf-

ficient ionic strength to suppress any polyelectrolyte effects. A value of 1.6 was evaluated for spheres, reducing to $\sim 0.2$ for long rod shape molecules.

Lavrenko and coworkers [10] also examined in detail the effects of free draining of solvent during macromolecular motion, demonstrating that this also had the effect of lowering $k_s/[\eta]$. A hydrodynamic intra-chain interaction or "draining" parameter has been defined [108] with limits $X = \infty$ for the non-free draining case and $X = 0$ for the free-draining case. A relation was given between $k_s/[\eta]$ and $X$ [10, 108]:

$$\{k_s/[\eta]\} = 8X/(3 + 8X) \tag{21}$$

This relation evidently leads to theoretical limits for $k_s/[\eta] = 0$ for free draining and 1 for non-free draining. The consequences of this are that unless the draining characteristics of the chain are properly known one has to be cautious in making conclusions about particle asymmetry, since it has been claimed that draining affects can mimic increase in asymmetry in lowering the $k_s/[\eta]$. Notwithstanding, many non-spherical molecules have empirical values for $k_s/[\eta]$ greater than 1.0: pullulans for example, considered as a random coil have been shown to have $k_s/[\eta] \sim 1.4$ (see [80]). Berth and coworkers [109] have argued that the very low $k_s/[\eta]$ values for chitosans are due to draining effects rather than a high degree of extension. Lavrenko and coworkers [10] have compiled an extensive list of $k_s/[\eta]$ values for a large number of other polysaccharides, complementing a list given by Creeth and Knight [107]: values are seen to range from 0.1 (potato amylose in 0.33 M KCl) to 1.8 (a cellulose phenylcarbamate in 1,4 dioxane), with some polysaccharides showing a clear dependence on molecular weight.

## 6.2 Power Law or Scaling Relations

The relation linking the sedimentation coefficient with the molecular weight for a homologous polymer series given above is (see [61, 111]):

$$s^0 = K'' M^b \tag{13}$$

(nb Lavrenko and coworkers [10] call the exponent $1 - b$). This relation is similar to the well-known Mark–Houwink–Kuhn–Sakurada relation linking the intrinsic viscosity with molecular weight:

$$[\eta] = K' M^a \tag{22}$$

and also a relation linking the radius of gyration $R_g$ with molecular weight.

$$R_g = K''' M^c \tag{23}$$

The power law or "MHKS" exponents $a, b, c$ have been related to conformation [61, 62] (Table 5).

**Table 5** Power Law exponents (from [61])

| | *a* | *b* | *c* |
|---|---|---|---|
| Sphere | 0 | 0.67 | 0.33 |
| Coil | 0.5–0.8 | 0.4–0.5 | 0.5–0.6 |
| Rod | 1.8 | 0.15 | 1.0 |

The coefficients in Table 5 correspond to the non-draining case. If draining effects are present then these will change the values for $a$ and $b$ – see, for example [110]. For example it has been shown that $a$ varies from 0.5 (non-draining case) to 1 (draining), again mimicking the effects of chain elongation. For homologous, linear types of polymer the power law indices are intercorrelated by the relations given by Tsvetkov, Eskin and Frenkel [62]:

$$b \sim (1 - c), \quad a \sim (2 - 3b) \quad \text{and} \quad c \sim (a + 1)/3 \tag{24}$$

Another scaling relation exists between the sedimentation coefficient and $k_s$ [see [10]]

$$k_s = K''''(s^0)^{æ} \tag{24a}$$

Lavrenko et al give æ and $K'''$ for a range of polysaccharides [10].

Various relations have been proposed linking the various power law exponents for a homologous series under specified conditions [10, 62] such as:

$$æ = (2 - 3b)/b \tag{25}$$

### 6.2.1 General Conformation: Haug Triangle and Conformation Zoning

Delineation of the three general conformation extremes (random coil, compact sphere, rigid rod) as indicated by the simple power or scaling laws and Wales–van Holde ratio, have been conveniently represented in the well-known Haug triangle (Fig. 8, see [61]). An extension of this idea was given by Pavlov et al. [112, 113]) who suggested five general conformation types or "zones", all of which could be distinguished using sedimentation measurements. The zones were: A (extra rigid rod), B (almost rigid rod), C (semi-flexible coil), D (random coil), E (globular/branched). A and B are distinguished by B having a very limited amount of flexibility. The zones were constructed empirically using a large amount of data ($s$, $k_s$) accumulated for polysaccharides of "known" conformation type, and plotted a scaling relation normalised with mass per unit length ($M_L$) measurements. (Fig. 9) The latter parameter can be obtained from knowledge of molecular weight from sedimentation equilibrium or light scattering and the chain length $L$ from small

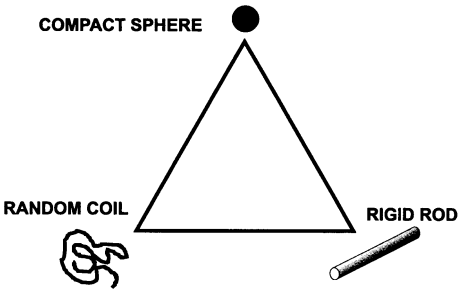


**Fig. 8** The Haug triangle. The three extremes of conformation (*compact sphere, random coil* and *rigid rod*) are placed at the apices of a triangle. The conformation of a given macromolecule is represented by a locus along the sides of the triangle between these extremes. Knowledge of the power law exponents (see text) can help to give us an idea of the conformation type. From [61]

angle X-ray scattering, X-ray fibre diffraction or high resolution NMR: Pavlov and colleagues give a comprehensive comparison of methods for heparin [5]. If the molecular weight is known, $M_L$ can also be estimated from electron microscopy [114]. Measurement of a data set $(s, k_s, M_L)$ of any target polysaccharide would then establish its conformation type. The limiting slopes of $\sim 4$ (extra rigid rod) and $\sim 0$ (globular/sphere) were shown to be theoretically reasonable. It should be stressed that this procedure is only a guide to conformation type. Along with other procedures using $k_s$ for conformation studies it assumes that charge contributions to the concentration have been suppressed by the supporting electrolyte, and also that draining effects are not significant or similar for the target polysaccharide and those polysaccharides whose data were used to set up the zones. Other normalised scaling relations have been suggested based on viscometry methods [113].

## 6.3 Rigid Cylindrical Structures

Once a general conformation type or "preliminary classification" has been established it is possible to use sedimentation data to obtain more detailed information about polysaccharide conformation. For example, the low value of $k_s/[\eta] \sim 0.25$ found for the bacterial polysaccharide xylinan has been considered to be due to asymmetry [115]. If we then assume a rigid structure the approximate theory of Rowe [36, 37] can be applied in terms of a prolate ellipsoid of revolution to estimate the aspect ratio $p$ ($\sim L/d$ for a rod, where $L$ is the rod length and $d$ is its diameter) $\sim 80$.

For a cylindrical rod an expression also exists for the sedimentation coefficient [116]:

$$s^0 = \{M(1 - \overline{v}\rho_0)/(3\pi\eta_0 N_A L)\} \cdot \{\ln(L/d) + \gamma\} \quad (26)$$

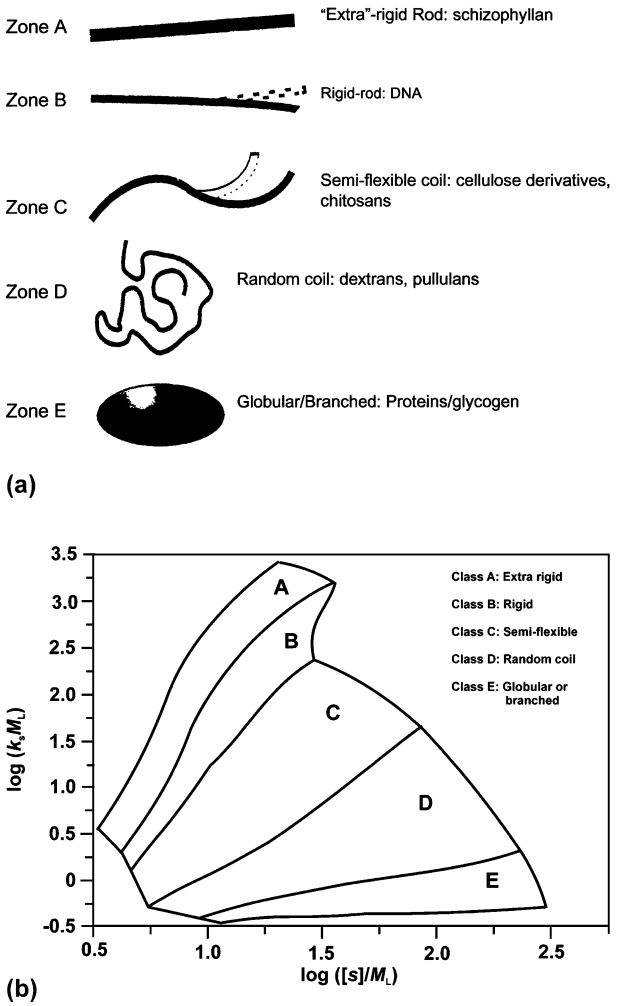


**Fig. 9** Conformation zoning of polysaccharide. **a** Conformation zones **b** Empirical plots for various polysaccharides of known conformation type used to form the zone plot. Measurement of $s$, $k_s$ and $M_L$ for a target polysaccharide will then help define its conformation zone or type. Redrawn and based on [112, 113]

where $\gamma$ is a function of $p$ and has a limiting value of $\sim 0.386$ for very long rods ($p \to \infty$). Replacing $L$ by the (molar) mass per unit length $M_L = M/L(\mathrm{g\,mol^{-1}\,cm^{-1}})$ this becomes

$$s^0 = \{M_L(1 - \overline{v}\rho_0)/(3\pi\eta_0 N_A)\} \cdot \{\ln M - \ln M_L - \ln d + \gamma\} \quad (27)$$

For the cases of finite $p$ (in the range 2–20) the currently accepted expression for $\gamma(p)$ is that of Tirado and Garcia de la Torre [117]

$$\gamma(p) = 0.312 + (0.561/p) + (0.100/p^2) \tag{28}$$

Above $p > 10$ the limiting value ($\gamma = 0.386$) can be used.

From Eqs. 27 and 28 we can obtain an estimate for the rod length $L$ if we know $M$ or $M_L$ (see above discussion) and have an estimate for the diameter $d$. As pointed out by Garcia de la Torre [118] the choice for $d$ is not so critical since it comes into the equations as the logarithm. It applies only to polysaccharides which are known to be rods.

## 6.4 Semi-Flexible Chains: Worm-Like Coils

Most linear polysaccharides are not rigid rods at all but are semi-flexible structures. The conformation and hydrodynamics of semi-flexible chains are most usefully represented by worm-like chains (see [119–122]), in which the bending flexibility is represented by the persistence length $L_\mathrm{p}$. This is an intrinsic property of a linear macromolecule: the greater the $L_\mathrm{p}$ the greater the rigidity and vice verse. More precisely, the conformation and flexibility of a macromolecular chain depends directly on $L/L_\mathrm{p}$, the ratio of the contour length to the persistence length. For $L/L_\mathrm{p} \ll 1$ the conformation is rod-like and Eqs. 26–28 can be applied. For $L/L_\mathrm{p} \gg 0$ the conformation approaches that of a random coil [119–122]. This can be best seen from the dependence of the radius of gyration on chain length, as clearly described by Freire and Garcia de la Torre [122]:

$$R_\mathrm{g}^2 = \{L \cdot L_\mathrm{p}/3\} \cdot \left\{1 - (3L/L_\mathrm{p}) + \left(6L_\mathrm{p}^2/L^2\right) + 6\left(L_\mathrm{p}^3/L^3\right)\left(1 - \mathrm{e}^{-L/L_\mathrm{p}}\right)\right\} \tag{29}$$

In the limit $L_\mathrm{p}/L \sim 0$, $R_\mathrm{g}$ is proportional to $L^{1/2}$ (n.b. this is misprinted in [122])—the classical dependence for a random coil—whereas when $L_\mathrm{p}/L \gg 1$, the classical relation for a rod is obtained: $R_g = L/\sqrt{12}$.

The sedimentation coefficient for wormlike chains was first worked out by Hearst and Stockmayer [123], later improved by Yamakawa and Fujii [124] to give this expression for $s^0$:

$$s^0 = \{M(1 - \overline{v}\rho_0)/(3\pi\eta_0 N_\mathrm{A} L)\} \cdot \left\{1.843 \ln(L/2L_\mathrm{p})^{1/2} + \alpha_2 + \alpha_3(L/2L_\mathrm{p})^{-1/2} + \ldots\right\} \tag{30}$$

If the persistence length $L_\mathrm{p}$ is much larger than the mean chain diameter, $d$, Yamakawa and Fujii gave limiting values for $\alpha_2 = -\ln(d/2L_\mathrm{p})$ and $\alpha_3 = 0.1382$. Freire and Garcia de la Torre [122] have considered further these coefficients. The factor $2L_\mathrm{p}$ appears rather than $L_\mathrm{p}$ simply because $2L_\mathrm{p}$ is equivalent to the statistical Kuhn segment length $\lambda^{-1}$.

A fundamental problem with the sedimentation coefficient is that it is the least sensitive parameter to conformation when compared with the intrinsic viscosity $[\eta]$ and the radius of gyration $R_g$. This lower sensitivity is offset by the ease of measurement and the ability to obtain $s^0$ to a higher accuracy (to better than 1%) compared with the other parameters. Nonetheless it is advisable not to use $s$ in isolation but in conjunction with $R_g$ and $[\eta]$ vs. $M$: two recent examples are a comparative study using ultracentrifugation, viscometry and light scattering on the relative conformations and flexibilities of galactomannans (guar, tara gum and locust bean gum), after pressure assisted solubilisation procedures [49] and a study using ultracentrifugation, viscometry and small angle X-ray scattering to investigate the conformation and flexibility of heparin [5].

## 7 Associative Interactions

There are many instances where associative interactions involving polysaccharides, whether they be self-association, complex formation or with small ligands are important (see [1]). Examples of self-association are dimerisation or trimerisation of helical types of polysaccharides, such as schizophyllan, scleroglucan (we could also mention xanthan and $\kappa$-carrageenan although that has been the subject of some disagreement). Examples of complex formation include the use of cellulose derivatives as dental adhesives, and an example of small ligand interactions is the intercalation of iodine by amylose or amylopectin. There has been considerable attention focussed on the use of polysaccharide systems as encapsulation agents for flavours and drugs, and this invokes both macromolecular and small ligand interactions involving polysaccharides [1]. The following Chapter by Muzzarelli and Muzzarelli [125] refers to a large number of these and other types of interactions involving the polycationic chitosan family of polysaccharides.

The analytical ultracentrifuge would appear to offer considerable potential for the analysis of these and other types of interaction. Indeed one of the main reasons behind the renaissance of analytical ultracentrifugation in the 1990s [126, 127] was the simmering need by molecular biologists and protein chemists for non-invasive solution based methods for studying biomolecular interactions, particularly the weaker ones involved in molecular recognition phenomena (see, e.g., [128, 129]). The analytical ultracentrifuge, its clean, medium free (no columns or membranes) and absolute nature has indeed proven a highly attractive tool for characterising the stoichiometry, reversibility and strength (as represented by the molar dissociation constant, $K_d$) of an interaction between well-defined systems: protein-protein, protein-DNA, protein-small ligand [2]. With polysaccharides we are generally dealing with

a different situation. Firstly, a polysaccharide does not have a single, clearly defined molecular weight: it is polydisperse with a distribution of molecular weights. Secondly, weak interactions ($K_d > 50\ \mu M$)—at least as far as we know—do not play a crucial functional role with polysaccharides as they do with proteins. Interactions, particularly involving polyelectrolytes of opposite charge (chitosan-alginate for encapsulation systems, chitosan-DNA for gene therapy) tend to be very strong or irreversible: the complexes tend to be much larger than for the simple associative protein-protein interactions. This means the main ultracentrifuge tool used for investigating protein-protein interactions, namely sedimentation equilibrium, has only limited applicability: sedimentation equilibrium has an upper limit of molecular weight of $\sim 50$ million g/mol. Examples of the use of the analytical ultracentrifuge to assay interactions involving polysaccharides include a study on mixtures of alginate with bovine serum albumin [130, 131], a study of galactomannan incubated with gliadin (as part of an ongoing investigation into the possible use of galactomannans to help intestinal problems) [132], chitosan with lysozyme [133] and synergistic interactions involving xanthan [134].

Polysaccharides can regulate weak interactions between protein molecules. A recent example is the effect of low molecular weight heparin molecules on the weak dimerisation of the plasminogen growth factor NK1, or at least a mutant thereof [135].

For large irreversible complexes involving polysaccharides a more valid assay procedure is to use sedimentation velocity (which can cope with complexes as large as $10^9$ g/mol), with the change in sedimentation coefficient ($s$, normalised to standard conditions or not) as our marker for complex formation. If we so wish we can then convert this to a change in molecular weight if we assume a conformation and use the power law relation (Eq. 13). Alternatively, we can simply use $s$ directly as our size criterion (this is not unusual: it is used for example in ribosome size representations, 30S, 50S etc., or in seed globulin, the 7S, 11S soya bean globulins etc [136, 137]).

## 7.1 Polysaccharide Mucoadhesive Interactions

A good example of where sedimentation velocity has played a valuable role in assaying large polysaccharide complexes is in the assessment of polysaccharides as mucoadhesives [138–143]: a drug administered orally or nasally tends to be washed away from the site of maximum absorption by the bodies natural clearance mechanisms before being absorbed. Incorporating the drug into a polysaccharide material which interacts with epithelial mucus in a controllable way has been proposed as a method of increasing the residence time and enhancing the absorption rate. The key macromolecule in mucus is mucin glycoprotein—a linear polypeptide backbone with linked saccharide chains to the extent that > 80% of the molecule is carbohydrate [63].

The carbohydrate has sites for ionic interaction (clusters of sialic acid or sulphate residues) and also hydrophobic interaction (clusters of hydrophobic methyl groups offered by fucose residues). Sedimentation velocity has been a valuable tool in the selection of appropriate mucoadhesives and in the characterisation of the complexes [138–143].

The approach is to first of all obtain mucin to a high degree of purity and to characterise the mucin and potential mucoadhesive. This is done by sedimentation velocity [$g^*(s)$] analysis and sedimentation equilibrium ($M^*$) analysis—according to the procedures described above—together with SEC-MALLs [145, 146].

The reactants are then mixed in various proportions, and the sedimentation ratio ($s_{complex}/s_{mucin}$)—the ratio of the sedimentation coefficient of the complex to that of the pure mucin itself—is used as the measure for mucoadhesion. The ultra-violet absorption optics on the XL-A or XL-I ultracentrifuge have been used as the main optical detection system. Although the polysaccharide is generally invisible in the near UV ($\sim 280$ nm), at the concentrations normally employed the mucin—in uncomplexed and complexed form—is detectable.

## 7.2 Mucoadhesion Involving Guar, Alginate, Carboxymethyl Cellulose, Xanthan and DEAE-Dextran

Experiments on a series of neutral and polyanionic polysaccharides revealed no significant change in the sedimentation coefficient (sedimentation ratio $s_{complex}/s_{mucin} \approx 1$) [138, 140, 141, 143] reinforcing macroscopic observations on whole mucus using tensiometry [147]. The polycationic derivative DEAE-dextran gave sedimentation ratios of 1.1–1.9 [138, 140, 141, 143] (Table 6) depending on the mixing ratio and temperature. This was rather modest considering the high charge density on the polymer with lots of potential sites for interaction with the ionized sialic acid groups on the mucin. This disappointment also reflects the disappointing result from the tensiometry analyses [147]. The $\alpha(1 \rightarrow 3)$ branches of the dextran appear to be responsible for considerable steric hindrance, preventing access to the charged mucin groups.

## 7.3 Mucoadhesion Experiments Involving Chitosans

A contrasting picture is seen for chitosans. Chitosans—as considered in detail in the following Chapter—are derivatives of chitin (after an alkali extraction procedure) and are available in large quantities from the shells of crabs, lobsters and other crustaceans. Pure chitin is poly-*N*-acetylglucoasmine. The *N*-acetyl groups are de-acetylated in chitosan to an extent represented by ei-

**Table 6** Sedimentation coefficient ratio. ($s_{complex}/s_{mucin}$) as an index of adhesiveness (Based on data from [138, 140, 143, 145])

| Polysaccharide mucoadhesive | $s_{complex}/s_{mucin}$ | Conditions |
|---|---|---|
| Alginate | 1 | pH 6.8, 20 °C |
| Carboxmethyl cellulose | 1 | pH 6.8, 20 °C |
| Guar | 1 | pH 6.8, 20 °C |
| Xanthan | 1 | pH 6.8, 20 °C |
| DEAE-dextran | 1.1–1.9* | pH 6.8, 20 °C |
| | 1.2–1.4* | pH 6.8, 37 °C |
| Chitosan ($F_A \approx 0.11$) | 48 | pH 6.5, 20 °C |
| | 34 | pH 6.5, 37 °C |
| | 15 | pH 4.5, 20 °C |
| | 38 | pH 4.5, 37 °C |
| | 22 | pH 2.0, 20 °C |
| | 12 | pH 2.0, 37 °C |
| | 26 | pH 4.5, 20 °C + 3 mM bile salt |
| | 35 | pH 4.5, 37 °C + 3 mM bile salt |
| | 18 | pH 4.5, 20 °C + 6 mM bile salt |
| | 14 | pH 4.5, 37 °C + 6 mM bile salt |
| Chitosan ($F_A \approx 0.42$) | 31 | pH 4.5, 20 °C |
| | 44 | pH 4.5, 37 °C |

*Depending on the mixing ratio

ther the degree of deacetylation or the degree of acetylation, $F_A$, with $F_A = 1$ being pure chitin and $F_A = 0–0.6$ representing the range of soluble chitosans. We stress here that chitosans are only readily soluble at pH values of 6.5 or less, and this factor has to be borne in mind in the formulation of any mucoadhesive product involving these substances (see [125]). Interestingly, whereas mucins present two types of residue for potential mucoadhesive interaction (the charged acidic groups on sialic acid and any sulphonated residues, and the hydrophobic methyl groups on fucose residues) chitosans present a similar opportunity (the charged $NH_3^+$ groups on deacetylated *N*-acetyl groups and also the hydrophobic acetyls on non-deacetylated residues). The results are quite spectacular [138–145] (Table 6). A highly charged chitosan ("sea cure" 210+) of $F_A \sim 0.11$ has impressive sedimentation ratios of 15–38 depending on the temperature. Interestingly for a lower-charged chitosan of $F_A \sim 0.42$, values of 31–44 were returned, reinforcing the view that both electrostatic and hydrophobic effects are important. The demonstration of large-size interaction products by the analytical ultracentrifuge used in this manner is reinforced by images from the powerful imaging techniques of electron microscopy and atomic force microscopy. Conventional transmission electron microscopy clearly demonstrates large complexes of the order of

$\sim 1\,\mu$m in size [148], and if we label the chitosan with gold we can see that the chitosan is distributed throughout the complex with "hot spots" in the interior [149]. Images from atomic force microscopy, visualized in topographic and phase modes, again shows complexes of this size. Control experiments revealed a loose coiled structure for pig gastric mucin and a shorter, stiffer conformation for the chitosan, consistent with solution measurements [150].

## 7.4 Effect of the Environment on the Extent of Interaction

The beauty of the analytical ultracentrifuge is that since it is a pure solution technique with no columns or membranes it allows us to easily alter the surrounding solvent conditions. For example [138, 140], if we vary the pH we see that the sedimentation ratio is $\sim 34$–$48$ at pH $\sim 6.5$ but is still significant at pH 2.0 ($s_{\text{complex}}/s_{\text{mucin}} \sim 12$–$22$: Table 6), below the *pKa* of the sialic acid groups on the mucin—which not only suggests the importance of the electrostatic contribution but indicates the existence of significant hydrophobic types of interaction. Attempts to investigate the effects of bile salts and differing ionic strengths down the alimentary tract also yield very much the same picture [138, 140]. At 0 mM bile salt $s_{\text{complex}}/s_{\text{mucin}}$ was found to be $\sim 18$–$21$, whereas at 6 mM the interaction is still significant, with $s_{\text{complex}}/s_{\text{mucin}} \sim 14$–$18$.

## 7.5 Sedimentation Fingerprinting

We would dearly love to perform these types of experiments on human small intestinal mucin if we could only get them in sufficient quantities in purified form. There has, however, been success in performing experiments on human mucin extracted from different parts of the stomach, namely the cardia, corpus and antrum regions. Although available in miniscule quantities we can assay mucoadhesiveness of chitosan on these by using a modification of the approach using the analytical ultracentrifuge described above, called Sedimentation Fingerprinting. In this method, introduced six years ago [151], the Schlieren optical system is used to record the concentration (refractive index) gradient $\mathrm{d}n/\mathrm{d}r$ as a function of radial position $r$ in the ultracentrifuge cell. The area under a "Schlieren peak" provides a measure of the sedimenting concentration. Alternatively, if interference optics on the XL-I ultracentrifuge are used, the area under a $g^*(s)$ versus $s$ plot would provide similar concentration information. Although the mucins from a human stomach are at too low a concentration to be detected we can assay for interaction from the loss of area under the chitosan peak caused by interaction. In this way Deacon and coworkers [151] showed it was possible to demonstrate significant differences in mucoadhesive interactions for different

regions of the stomach (Fig. 10). This type of information obtained with the ultracentrifuge reinforced with other data is helping us design effective mucoadhesive systems. An example is the use of tripolyphosphate to cross-link chitosan into a sphere [152]: if this is done in the presence of a drug, the drug can be encapsulated. Tripolyphosphate-linked chitosans have been shown to give good mucoadhesion [153], and although nothing has been published yet the principle of co-sedimentation could be used as a successful assay here as it has been in the assay of non-polysaccharide-based encapsulation systems [153, 155]. This and other aspects are considered in a recent review on mucoadhesion [138].

## 7.6 Measurement of Charge and Charge Screening

The final application we would like to highlight is a recent application of the analytical ultracentrifuge to our understanding of the behaviour of polysaccharides in solution is the measurement of charge on polyelectrolyte polysaccharides, and the extent of charge screening through interaction with low molecular weight electrolyte [14]. In recent years there has been a tendency to identify the charges on polysaccharides and polynucleotides with the values calculated from the chemical structure. However, the phenomenon of charge-screening (or counterion condensation) has long been an established feature of polyelectrolyte theory [156–158]. Relatively small magnitudes of the effective net charges of polysaccharides [159–161] and other carbohydrate-based polymers with a significant amount of charged groups—such as nucleic acids [162, 163]—afford examples with direct relevance to biology.

Winzor and coworkers have employed measurements of the Donnan distribution of small ions in dialysis equilibrium [14] to reinforce earlier evidence of charge-screening effects in polysaccharide anions [164, 165]. These researchers used the absorption optical system of a Beckman XL-I ultracentrifuge to monitor the distribution of ions in polysaccharide solutions

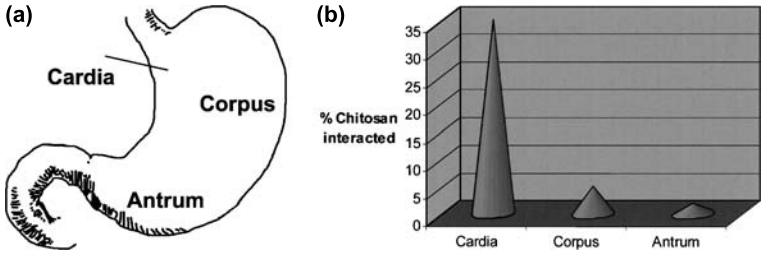


**Fig. 10** Sedimentation analysis of the comparative mucoadhesiveness of a chitosan (sea cure 210+, $F_A \sim 0.11$) to mucins from different parts of the stomach **a** Mucin source **b** Histogram. Adapted from [151]

dialyzed against sodium phosphate buffer (pH 6.8, I 0.08) supplemented with 0.2 mM chromate as an indicator ion. Three polyanionic polysaccharides were chosen for analysis. After extensive dialysis against the same chromate-supplemented buffer to establish the Donnan equilibrium distribution of small ions the difference between chromate concentrations in the polysaccharide and diffusate solutions was monitored by means of the absorption optical system: the ultracentrifuge is merely being used as a double-beam spectrophotometer when a sufficiently low speed (3000 rpm) is used to ensure uniformity of solution composition throughout the cell. As in classical difference spectroscopy, diffusate was placed in the reference sector of the cell to allow direct measurement of the absorbance difference from a scan at 375 nm.

In equilibrium dialysis of a solution of a polyanion (valence $Z_P$ negative) with molar concentration $C_P$ against a solution of uni-univalent electrolyte CA (C = cation, A = anion) with molar concentration $C_{CA}$ it was shown that the requirement for equal chemical potentials of the salt in the polyanion ($\alpha$) and diffusate ($\beta$) phases results in the following relation

$$\left(\gamma_{\pm}^{\alpha}/\gamma_{\pm}^{\beta}\right)\left(C_i^{\alpha}/C_i^{\beta}\right)^{1/Z_i} = 1 - Z_P C_P^{\alpha}/(2I^{\beta}) + \ldots \tag{31}$$

Comparison of the concentrations of either the cation or the anion in the two phases thus has potential for evaluating the polyanion valence provided that estimates of the mean ion activity coefficient ($\gamma_{\pm}$) are available. Furthermore, as realized by Svensson [165], expression of the Donnan distribution of small ions in this manner has two advantages in that (i) Eq. 31 applies to each type of small ion in situations where the supporting electrolyte is not restricted to single cationic and anionic species; and (ii) multivalence of a small ion is also accommodated.

In a typical equilibrium dialysis study of charged polysaccharides an indicator ion, L (chromate), is included in the supporting electrolyte medium (phosphate buffer, pH 6.8, I 0.08) to allow assessment of the effective net charge of the polyanions via a modified form of Eq. 31, namely,

$$\left(C_L^{\alpha}/C_L^{\beta}\right)^{1/Z_L} = 1 - fZ_P C_P/(2I^{\beta}) + \ldots \tag{32}$$

where $Z_L$ is the chromate valence (– 2). The factor $f$ is included to allow expression of the effective net charge as a fraction of the nominal valence $Z_P$ that is indicated by the chemical structure of the saccharide repeat unit: $f = Z_{eff}/Z_P$.

For dextran sulphate, heparin and polygalacturonate the effective net charges were shown by Winzor and coworkers to be only one-third ($f \sim 0.3$) of those deduced from the chemical structures [14]—a reflection of charge screening (counterion condensation) in aqueous polyelectrolyte solutions. Whereas the extent of charge screening for the first two polysaccharides agrees well with theoretical prediction, the disparity in the corresponding comparison for polygalacturonate was deemed to reflect partial esterifica-

tion of carboxyl groups, whereupon the experimental parameter refers to the effective charge per hexose residue rather than the effective fractional charge of each carboxyl group. It is therefore wrong to calculate the charge on a polysaccharide in solution on the basis merely of the numbers or number density of charged residues like $COO^-$ or $SO_3^{2-}$, even in cases where the pH is such that the groups are fully ionised.

## 8 Comment

The analytical ultracentrifuge has emerged from its Cinderella status as for polysaccharide characterisation, catalyzed by the new generation instrumentation with on-line data capture and some major advances in software for data capture and analysis. In a review article written a decade ago [12] it was predicted that the imminent launch of the XL-I ultracentrifuge would have a considerable impact with regards sedimentation velocity analysis of polysaccharide heterogeneity, polydispersity and conformation. This has indeed been the case. The role of the ultracentrifuge for sedimentation equilibrium analysis of polysaccharide molecular weight is still very important, but more as providing a valuable independent check on the reliability of results coming out of SEC/MALLs. It has been shown to have considerable potential for the analysis of interactions involving polysaccharides, even though the types of interaction involved are quite different from the better defined reversible types of interaction encountered in protein biochemistry where analytical ultracentrifugation has made a huge impact. One would therefore infer that an analytical ultracentrifuge would be a valuable part of the armoury of any researcher interested in understanding the size, conformation and interaction properties of polysaccharides in the environment where many occur naturally—in the solution state. And there is no need for columns or membranes or a requirement to immobilise material onto a surface: it is a free solution technique. Its versatility is even more impressive: this article has only focussed on its use for analysis of solutions: we haven't touched upon its uses for the analysis of the rheological and thermodynamic properties of polysaccharide gels [15], phase diffusion and interfacial transport phenomena involving polysaccharides [16], and the formation of films and membranes [17].

## References

1. Tombs MP, Harding SE (1997) An Introduction to Polysaccharide Biotechnology. Taylor and Francis, London
2. Harding SE, Rowe AJ, Horton JC (eds) (1992) Analytical Ultracentrifugation in Biochemistry and Polymer Science. Royal Society of Chemistry, Cambridge, UK

3. Burchard W (1992) In: Harding SE, Sattelle DB, Bloomfield VA (eds) Laser Light Scattering in Biochemistry. Royal Society of Chemistry, Cambridge, UK, 3
4. Wyatt PJ (1992) In: Harding SE, Sattelle DB, Bloomfield VA (eds) Laser Light Scattering in Biochemistry. Royal Society of Chemistry, Cambridge, UK, 35
5. Pavlov G, Finet S, Tatarenko K, Korneeva E, Ebel C (2003) Eur Biophys J 32:437
6. Harding SE (1997) Prog Biophys Mol Biol 68:207
7. Van der Merwe A (2001) In: Harding SE, Chowdhry BZ (eds) Protein-Ligand Interactions: Hydrodynamics and Calorimetry. Oxford University Press, Oxford, UK, 137
8. Lapasin R, Pricl S (1995) Rheology of Industrial Polysaccharides. Theory and Applications. Blackie, London
9. Harding SE (1992) In: Harding SE, Rowe AJ, Horton JC (eds) Analytical Ultracentrifugation in Biochemistry and Polymer Science. Royal Society of Chemistry, Cambridge, UK, 495
10. Lavrenko PN, Linow KJ, Görnitz E (1992) In: Harding SE, Rowe AJ, Horton JC (eds) Analytical Ultracentrifugation in Biochemistry and Polymer Science. Royal Society of Chemistry, Cambridge, UK, 517
11. Harding SE (1993) Gums and Stabilisers for the Food Industry 8:55
12. Harding SE (1995) Carbohyd Polym 28:227
13. Jumel K, Fiebrig I, Harding SE (1996) Int J Biol Macromol 18:133
14. Winzor DJ, Carrington LE, Deszczynski M, Harding SE (2004) Biomacromolecules 5:2456
15. Cölfen H (1999) Biotech Genet Eng Rev 16:87
16. Harding SE, Tombs MP (2002) Biotech Genet Eng Rev 19:55
17. Wandrey C, Grigorescu G, Hunkeler D (2002) Prog Colloid Polym Sci 119:91
18. Jullander I (1987) In: Ranby B (ed) Physical Chemistry of Colloids and Macromolecules. The Svedberg Symposium. Blackwell Scientific, Oxford, UK, 29
19. Schachman (1992) In: Harding SE, Rowe AJ, Horton JC (eds) Analytical Ultracentrifugation in Biochemistry and Polymer Science. Royal Society of Chemistry, Cambridge, UK, 3
20. Görnitz E, Linow KJ (1992) In: Harding SE, Rowe AJ, Horton JC (eds) Analytical Ultracentrifugation in Biochemistry and Polymer Science. Royal Society of Chemistry, Cambridge, UK, 26
21. Giebeler R (1992) In: Harding SE, Rowe AJ, Horton JC (eds) Analytical Ultracentrifugation in Biochemistry and Polymer Science. Royal Society of Chemistry, Cambridge, UK, 16
22. Errington N, Harding SE, Rowe AJ (1992) Carbohyd Polym 17:151
23. Errington N, Harding SE, Illum L, Schacht E (1992) Carbohyd Polym 18:289
24. Cölfen H, Harding SE, Vårum KM (1996) Carbohyd Polym 30:5
25. Furst AJ (1997) Europ Biophys J 25:307
26. Theisen C, Johann C, Deacon MP, Harding SE (2000) Refractive Increment Data Book for Polymer and Biomolecular Scientists. Nottingham University Press, Nottingham, UK
27. Anthonsen MW, Vårum KM, Smidsrød O (1993) Carbohyd Polym 22:193
28. Preston BN, Wik KO (1992) In: Harding SE, Rowe AJ, Horton JC (eds) Analytical Ultracentrifugation in Biochemistry and Polymer Science. Royal Society of Chemistry, Cambridge, UK, 549
29. Majzoobi M (2004) PhD Thesis, University of Nottingham, Nottingham, UK
30. Schachman H (1959) Ultracentrifugation in Biochemistry. Academic Press, New York

31. Gibbons RA (1972) In: Gottschalk A (ed) Glycoproteins: Their Composition, Structure and Function. Elsevier, Amsterdam, 5A, 31
32. Kratky O, Leopold H, Stabinger H (1973) Meth Enzymol 27D:98
33. Laue TM, Shah BD, Ridgeway TM, Pelletier SL (1992) In: Harding SE, Rowe AJ, Horton JC (eds) Analytical Ultracentrifugation in Biochemistry and Polymer Science. Royal Society of Chemistry, Cambridge, UK, 90
34. http://www.jphilo.mailway.com/download.htm
and http://www.rasmb.bbri.org/rasmb/windows/sednterp-philo/
35. Gralén N (1944) Sedmentation and Diffusion Measurements on Cellulose and Cellulose Derivatives. PhD Thesis, University of Uppsala, Uppsala, Sweden
36. Rowe AJ (1977) Biopolymers 16:295
37. Rowe AJ (1992) In: Harding SE, Rowe AJ, Horton JC (eds) Analytical Ultracentrifugation in Biochemistry and Polymer Science. Royal Society of Chemistry, Cambridge, UK, 394
38. Fujita H (1962) Mathematical Theory of Sedimentation Analysis. Academic Press, New York
39. Fujita H (1975) Foundations of Ultracentrifugal Analysis. Wiley, New York
40. Stafford W (1992) In: Harding SE, Rowe AJ, Horton JC (eds) Analytical Ultracentrifugation in Biochemistry and Polymer Science. Royal Society of Chemistry, Cambridge, UK, 359
41. Philo JS (2000) Anal Biochem 279:151
42. Schuck P (1998) Biophys J 75:1503
43. Dam J, Schuck P (2004) Meth Enzymol (in press)
44. http://www.jphilo.mailway.com/download.htm
45. Lamm O (1923) Ark Mat Astr Fys 21B(2):1
46. Claverie JM, Dreux H, Cohen R (1975) Biopolymers 14:1685
47. http://www.analyticalultracentrifugation.com/download.htm
48. Harding SE (1995) Biophys Chem 55:69
49. Patel T, Picout DR, Parlov G, Garcia de la Torre J, Ross-Murphy SB, Harding SE (2005) mss. submitted
50. Svedberg T, Pedersen KO (1940) The Ultracentrifuge. Oxford University Press, Oxford, UK
51. Korneeva EV, Vichoreva GA, Harding SE, Pavlov GM (1996) Abstr Am Chem Soc 212(1):75-cell
52. Pavlov GM, Korneeva EV, Harding SE, Vichoreva GA (1998) Polymer 39:6951
53. Pavlov GM, Korneeva EV, Vikhoreva GA, Harding SE (1998) Polym Sci Ser A 40; and (1998) Vysokomolekulyarnye Soed Ser A 40:2048
54. Pavlov GM, Korneeva EV, Nepogod'ev SA, Jumel K, Harding SE (1998) Polym Sci Ser A 40:1282; and (1998) Vysokomolekulyarnye Soed Ser A 40:2056
55. Pavlov GM, Korneeva EV, Jumel K, Harding SE, Meyer EW, Peerlings HWI, Stoddart JF, Nepogodiev SA (1999) Carbohyd Polym 38:195
56. Sharman WR, Richards EL, Malcolm GN (1978) Biopolymers 17:2817
57. Igarishi O, Sakurai Y (1965) Agr Biol Chem 29:678
58. Djurtoft R, Rasmussen KL (1955) Eur Brew Conv Congress, p 17
59. Wedlock DJ, Fasihuddin BA, Phillips GO (1987) Food Hydrocolloids 1:207
60. Pusey PN (1974) In: Cummings HZ, Pike ER (eds) Photon Correlation and Light Beating Spectroscopy. Plenum Press, New York, 387
61. Smidsrød O, Andresen IL (1979) Biopolymerkjemi. Tapir, Trondheim, Norway
62. Tsvetkov VN, Eskin V, Frenkel S (1970) Structure of Macromolecules in Solution. Butterworths, London

63. Harding SE (1989) Adv Carbohyd Chem 47:345
64. Pain RH (1980) Symp Soc Exp Biol 34:359
65. Svedberg T, Fåhraeus R (1926) J Am Chem Soc 48:430
66. Clewlow AC, Errington N, Rowe AJ (1997) Eur Biophys J 25:305
67. Mächtle W (1999) Prog Coll Polym Sci 113:1
68. http://www.nottingham.ac.uk/ncmh
69. Harding SE, Horton JC, Morgan PJ (1992) In: Harding SE, Rowe AJ, Horton JC (eds) Analytical Ultracentrifugation in Biochemistry and Polymer Science. Royal Society of Chemistry, Cambridge, UK, 275
70. Cölfen H, Harding SE (1997) Eur Biophys J 24:333
71. Van Holde KE, Baldwin RL (1958) J Phys Chem 62:734
72. Yphantis DA (1964) Biochemistry 3:297
73. Creeth JM, Harding SE (1982) J Biochem Biophys Meth 7:25
74. Hall DR, Harding SE, Winzor DJ (1999) Prog Coll Polym Sci 113:62
75. Teller DC, Horbett JA, Richards EG, Schachman HK (1969) Ann New York Acad Sci 164:66
76. Creeth JM, Pain RH (1967) Prog Biophys Mol Biol 17:217
77. Minton AP (1994) In: Schuster TM, Laue TM (eds) Modern Analytical Ultracentrifugation. Birkhäuser, Boston, 81
78. http://www.nottingham.ac.uk/ncmh/unit/method.html#Software
79. http://vm.uconn.edu/~wwwbiotc/uaf.html
80. Kawahara K, Ohta K, Miyamoto H, Nakamura S (1984) Carbohyd Polym 4:335
81. Sato T, Norisuye T, Fujita H (1984) Macromolecules 17:2696
82. Woodward JR, Phillips DR, Fincher GB (1983) Carbohyd Polym 3:143
83. Edmond E, Farquhar S, Dunstone JR, Ogston AG (1968) Biochem J 108:755
84. Muzzarelli RAA, Lough C, Emanuelli M (1987) Carbohyd Res 164:433
85. Berth G, Dautzenberg H, Lexow D, Rother G (1990) Carbohyd Polym 12:39
86. Lecacheux D, Mustiere Y, Panaras R, Brigand G (1986) Carbohyd Polym 6:477
87. Yanaki T, Kojima T, Norisuye T (1981) Polym J 13:1135
88. Wedlock DJ, Baruddin BA, Phillips GO (1986) Int J Biol Macromol 8:57
89. Dhami R, Harding SE, Jones T, Hughes T, Mitchell JR, To K-M (1995) Carbohyd Polym 27:93
90. Harding SE, Day K Dhami R, Lowe PM (1997) Carbohyd Polym 32:81
91. Horton JC, Harding SE, Mitchell JR, Morton-Holmes DF (1991) Food Hydrocolloids 5:125
92. Straatman A, Borchard W (2002) Prog Coll Polym Sci 119:64–69
93. Harding SE (1985) Biophys J 47:247
94. Ball A, Harding SE, Mitchell JR (1988) Int J Biol Macromol 10:259
95. Harding SE, Berth G, Ball A, Mitchell JR, Garcia de la Torre J (1991) Carbohyd Polym 16:1
96. Herdan G (1949) Nature 163:139
97. Tombs MP, Peacocke AR (1974) The Osmotic Pressure of Biological Macromolecules. Clarendon Press, Oxford
98. Roark D, Yphantis DA (1969) Ann New York Acad Sci 164:245
99. Rinde H (1928) The Distribution of the Sizes of Particles in Gold Sols Prepared According to the Nuclear Method. PhD Thesis, University of Uppsala, Uppsala, Sweden
100. Harding SE (1988) Gums and Stabilisers for the Food Industry 4:15
101. http://www.wyatt.com/
102. Horton JC, Harding SE, Mitchell JR (1991) Biochm Soc Trans 19:510
103. Rollings JE (1991) Biochem Soc Trans 19:493

104. Rollings JE (1992) In: Harding SE, Sattelle DB, Bloomfield VA (eds) Laser Light Scattering in Biochemistry. Royal Society of Chemistry, Cambridge, UK, 275
105. Wolff D, Czapla S, Heyer AG, Radosta S, Mischnick P, Springer J (2000) Polymer 41:8009
106. Wales M, Van Holde KE (1954) J Polym Sci 14:81
107. Creeth JM, Knight CG (1965) Biochim Biophys Acta 102:549
108. Freed KF (1976) J Chem Phys 65:4103
109. Berth G, Cölfen H, Dautzenberg H (2002) Prog Coll Polym Sci 119:50
110. Pavlov GM (2002) Prog Coll Polym Sci 119:84
111. Harding SE, Vårum KM, Stokke BT, Smidsrød O (1991) Adv Carbohyd Analysis 1:63
112. Pavlov GM, Rowe AJ, Harding SE (1997) Trends Analyt Chem 16:401
113. Pavlov GM, Harding SE, Rowe AJ (1999) Prog Coll Int Sci 113:76
114. Stokke BT, Elgsaeter A (1991) Adv Carbohyd Analysis 1:195
115. Harding SE, Berth G, Hartmann J, Jumel K, Cölfen H, Christensen BE (1996) Biopolymers 39:729
116. Broesma S (1960) J Chem Phys 32:1626
117. Tirado MM, Garcia de la Torre J (1979) J Chem Phys 71:2581
118. Garcia de la Torre J (1992) In: Harding SE, Rowe AJ, Horton JC(eds) Analytical Ultracentrifugation in Biochemistry and Polymer Science. Royal Society of Chemistry, Cambridge, UK, 333
119. Yamakawa H (1971) Modern Theory of Polymer Solutions. Harper and Row, New York
120. Bloomfield VA, Crothers DM, Tinoco L (1974) Physical Chemistry of Nucleic Acids. Harper and Row, New York
121. Cantor CR, Schimmel PR (1979) Biophysical Chemistry. Freeman, New York
122. Freire JJ, Garcia de la Torre J (1992) In: Harding SE, Rowe AJ, Horton JC (eds) Analytical Ultracentrifugation in Biochemistry and Polymer Science. Royal Society of Chemistry, Cambridge, UK, 346
123. Hearst JE, Stockmayer WH (1962) J Chem Phys 37:1425
124. Yamakawa H, Fujii M (1973) Macromolecules 6:407
125. Muzzarelli RAA, Muzzarelli C (2005) Adv Polym Sci Heinze T (ed) (this volume)
126. Schachman HK (1989) Nature 941:259
127. Schachman HK (1992) In: Harding SE, Rowe AJ, Horton JC (eds) Analytical Ultracentrifugation in Biochemistry and Polymer Science. Royal Society of Chemistry, Cambridge, UK, 3
128. Watson JD (1970) The Molecular Biology of the Gene (2nd Edn). Benjamin, New York
129. Silkowski H, Davis SJ, Barclay AN, Rowe AJ, Harding SE, Byron O (1997) Eur Biophys J 25:455
130. Harding SE, Jumel K, Kelly R, Gudo E, Horton JC, Mitchell JR (1993) In: Schwenke KD, Mothes R (eds) Food Proteins: Structure and Functionality. VCH, Weinheim, Germany, 216
131. Kelly R, Gudo ES, Mitchell JR, Harding SE (1994) Carbohyd Polym 23:115
132. Seifert A, Heinevetter L, Cölfen H, Harding SE (1995) Carbohyd Polym 28:239
133. Cölfen H, Harding SE, Vårum KM, Winzor DJ (1996) Carbohyd Polym 30:45
134. Mannion RO, Melia CD, Launay B, Cuvelier G, Hill SE, Harding SE, Mitchell JR (1992) Carbohyd Polym 19:91
135. Bandyopadhyay A (2004) Structural Biology of the Plasminogen-related Growth Factors and their Receptors. PhD Thesis, University of Cambridge, Cambridge, UK

136. Schwenke KD (1985) Eiweißquellen der Zukunft. Urania-Verlag, Leipzig, German Democratic Republic
137. Prakash V (1992) In: Harding SE, Rowe AJ, Horton JC (eds) Analytical Ultracentrifugation in Biochemistry and Polymer Science. Royal Society of Chemistry, Cambridge, UK, 445
138. Harding SE (2003) Biochem Soc Trans 31:1036
139. Deacon MP (1999) Polymer Bioadhesives for Drug Delivery. PhD Thesis, University of Nottingham, Nottingham, UK
140. Harding SE, Deacon MP, Fiebrig I, Harding SE (1999) Biotech Gen Eng Rev 16:41
141. Fiebrig I, Davis SS, Harding SE (1995) In: Harding SE, Hill SE, Mitchell JR (eds) Biopolymer Mixtures. Nottingham University Press, Nottingham, UK, 373
142. Fiebrig I (1995) Solution Studies on the Mucoadhesive Potential of Various Polymers for use in Gastrointestinal Drug Delivery Systems. PhD Thesis, University of Nottingham, Nottingham, UK
143. Anderson MT, Harding SE, Davis SS (1989) Biochem Soc Trans 17:1101
144. Fee M (2004) Evaluation of Chitosan Stability in Aqueous Systems. PhD Thesis, University of Nottingham, Nottingham, UK
145. Fiebrig I, Harding SE, Davis SS (1994) Prog Coll Polym Sci 94:66
146. Jumel K, Fogg FJJ, Hutton DA, Pearson JP, Allen A, Harding SE Eur Biophys J 25:477
147. Lehr CM, Bouwstra JA, Schacht EH, Junginger HE (1992) Int J Pharmaceut 78:43
148. Fiebrig I, Harding SE, Rowe AJ, Hyman SC, Davis SS (1995) Carbohyd Polym 28:239
149. Fiebrig I, Vårum KM, Harding SE, Davis SS, Stokke BT (1997) Carbohyd Polym 33:91
150. Deacon MP, McGurk S, Roberts CJ, Williams PM, Tendler SJB, Davies MC, Davis SS, Harding SE (2000) Biochem J 348:557
151. Deacon MP, Davis SS, White RJ, Nordman H, Carlstedt I, Errington N, Rowe AJ, Harding SE (1999) Carbohyd Polym 38:235
152. Zengshuan MA, Yeoh HH, Lim LY (2002) J Pharm Sci 91:1396
153. He P, Davis SS, Illum L (1998) Int J Pharm 166:75
154. Davison CJ, Smith KE, Hutchinson LEF, O'Mullane JE, Harding SE, Brookman L, Petrak K (1990) J Bioactive Compatible Polym 5:7
155. Morgan PJ, Harding SE, Petrak K (1990) Macromolecules 23:4461
156. Katchalsky A, Alexandrowicz Z, Kedem O (1996) In: Conway BE, Barradas RG (eds) Chemical Physics of Ionic Solutions. Wiley, New York, 295
157. Manning GS (1969) J Chem Phys 51:924
158. Manning GS (1978) Q Rev Biophys 11:179
159. Braswell E (1968) Biochim Biophys Acta 158:103
160. Preston BN, Snowden JM, Houghton KT (1972) Biopolymers 11:1645
161. Comper WD, Preston BN (1974) Biochem J 143:1
162. Creeth JM, Jordan DO (1949) J Chem Soc 1409
163. Mathieson AR, Matty SJ (1957) Polym Sci 23:747
164. Adair GS, Adair ME (1934) Biochem J 38:199
165. Svensson H (1946) Ark Kemi Mineral Geol 22A(10):1